

EXPLORATION OF LOW SWAP (SIZE WEIGHT AND POWER)  
DIFFUSE OPTICAL TOMOGRAPHY AND IMAGING  
TECHNIQUE FOR BIOMETRICS

A THESIS  
IN  
Electrical Engineering

Presented to the Faculty of the University  
of Missouri–Kansas City in partial fulfillment of  
the requirements for the degree

MASTER OF SCIENCE

by  
TEJASWI DHANDU  
Kansas City, MO, USA

Kansas City, Missouri  
2023

© 2023

TEJASWI DHANDU

ALL RIGHTS RESERVED

EXPLORATION OF LOW SWAP (SIZE WEIGHT AND POWER)  
DIFFUSE OPTICAL TOMOGRAPHY AND IMAGING  
TECHNIQUE FOR BIOMETRICS

Tejaswi Dhandu, Candidate for the Master of Science Degree

University of Missouri–Kansas City, 2023

ABSTRACT

This paper introduces a novel vein-matching system that merges vein images and diffuse optical tomography (DoT) data. The study focuses on the successful creation of a compact and energy-efficient hardware system for Diffuse Optical Tomography (DoT) and vein imaging, two distinct biometric techniques. The vein imaging setup is composed of a near-infrared camera and an 870nm IR light source. The primary objective was to overcome the limitations associated with traditional imaging methods by devising a streamlined and effective hardware arrangement with reduced size, weight, and power consumption.

In pursuit of this aim, we constructed hardware setups from the ground up for both diffuse optical tomography and vein imaging. We explored inventive designs that incorporated 870nm infrared (IR) LEDs and IR sensors, predominantly photodiodes,

enabling the capture of significant data and enhancing overall image quality. The system's configuration underwent optimization based on parameters including light illumination, penetration depth, sensor input, and analog signal processing.

Consequently, the outcome is a set of portable biometric hardware systems that provide real-time access to both DoT and vein imaging functionalities. Empirical findings demonstrate that the proposed system achieves a remarkable level of matching accuracy and exhibits resilience in the face of environmental variations, including diverse lighting conditions and scenarios. This advancement represents a noteworthy progression in the biometrics field, enhancing adaptability and user-friendliness across a range of applications, such as security and human-computer interaction. The amalgamation of these two biometric approaches sets the stage for more precise and comprehensive acquisition of biometric data, effectively addressing the escalating demand for dependable and efficient biometric systems in varied domains.

## APPROVAL PAGE

The faculty listed below, appointed by the Dean of the School of Computing and Engineering, have examined a thesis titled “Exploration of Low SWaP (Size Weight and Power) Diffuse Optical Tomography and Imaging Technique for Biometrics” presented by Tejaswi Dhandu, a candidate for the Master of Science degree, and hereby certify that in their opinion it is worthy of acceptance.

### Supervisory Committee

Rahman Mostafizur, Ph.D., Committee Chair

Department of Division of Energy and Systems, UMKC

Preetham Goli, Ph.D.

Department of Division of Energy, matter, and systems, UMKC  
Committee Member 1

Mahbube K. Sidiki, Ph.D.

Department of Computer Science Electrical Engineering, UMKC  
Committee Member 2

## CONTENTS

ABSTRACT .....	iii
ILLUSTRATIONS .....	viii
TABLES .....	xiii
ACKNOWLEDGEMENTS .....	xii
CHAPTER 1 .....	1
1.1 Background .....	3
1.2 Problem Statement .....	5
1.3 Objectives .....	6
1.4 Limitations .....	7
1.5 Thesis Organization .....	8
CHAPTER 2 .....	9
HARDWARE DESIGN .....	9
2.1 DOT Hardware design .....	10
2.2 Vein Imaging System .....	16

CHAPTER 3 .....	24
TEST METHODOLOGY .....	24
3.1 IR IMAGING.....	24
3.2 DoT setup.....	30
CHAPTER 4 .....	35
RESULTS AND DISCUSSION.....	35
4.1 IR Imaging .....	36
4.2 DoT data.....	41
CHAPTER 5 .....	48
CONCLUSION AND FUTURE WORK.....	48
5.1 Conclusion .....	48
5.2 Future Work .....	49
REFERENCE LIST .....	51
VITA .....	56

## ILLUSTRATIONS

Figure	Page
1. Figure 1 Rectangular four-zonal PCB (A)outer view(B)top view. This initial setup intended to be used for both IR imaging and DoT setups. It consists of four PCBs in the shape of a rectangle mold with alternate arrangements of LEDs and Sensors and a space for a camera.....	12
2. Figure 2 Wristband with breadboard resembling FNIRs device (A)front view (B)back view. The wristband is made up of sensors and LEDs with high-power 870 nm LEDs, and the breadboard comprises resistors and ADCs that are powered by a Raspberry Pi. HDMI cable is used to connect the Raspberry Pi to the monitor.....	13
3. Figure 3 wristband with PCB.....	14
4. Figure 4 Wristband with customized PCB (A)customized PCB with resistors and ADCs soldered on it. Power supply from raspberry pi up to 5V (B)wristband with cluster of LEDs surrounding a sensor covered with diffusers for ambient light control.....	15
5. Figure 5 Breadboard setup. (A) setup connected on breadboard (B) connected on breadboard with LEDs turned on nighttime. Configuration [1] with breadboard setup with LEDs and resistors. Refracted image is capture by placing the LEDs and camera on each side of the wrist. reflected image is captured by placing camera and LEDs on same side of the wrist. ....	17
6. Figure 6 Four zonal PCB configuration. (A) four zonal setups with LEDs on the top bottom and sides of the wrist. Camera space on top view to capture images from top.	



hand inserted inside square. (B) Same piece of PCB on three sides of wrist: bottom, two sides. (C) top zone of the setup with camera space surrounded by LEDs. ....19

7. Figure 7 Modified 4 zone setup with camera hood. (A) wristband with PCB setup molded open (B) Setup molded just the way molded to the wrist (C) model showing how it is wrapped to hand (D) upper PCB holding the hood which holds the camera and upper illumination lights (E) how the camera holder is connected to the PC via Cable (F) Mini photo booth to capture images to avoid ambient light entering the setup .....21

8. Figure 8 Wristband with customized 3D holder. (A) the final configuration with wristband form factor and customized 3D module as camera holder and top illumination of the setup. Upper circle; inner view of holder and bottom circle; outer view of holder. (B) top view, the way setup is wrapped to wrist (C) side view of wrist after wrapping setup. ....23

9. Figure 9 3D Printed Phantom model using sketchfab.com. (A)Front view of the phantom(B)back view of the phantom.....25

10. Figure 10 Palmar and Dorsal side of the wrist. Top, left to right: Palmar side anterior views of musculature and nerve arcades, veins and arteries, skeletal patterns, and standard views of the hand and forearm. Dorsal side Bottom row depicts the corresponding posterior views. ....26

11. Figure 11 IR imaging setup.....28

12. Figure 12 Wristband with customized PCB Figure depicts a setup integrated with IR LEDs and sensors, power supply to R-pi and data conversion via ADCs for conducting DoT measurements. ....33

13. Figure 13 Phantom model and wristband results with breadboard connection. Results

with breadboard configuration captured at nighttime only made the veins visible on the palm, not on the wrist that was our aim. Intensity is insufficient. IR images of phantom with Exposure: 47498.609  $\mu$ s, Gain: 12.8dB (C) IR images of wrist with Exposure: 849040.870  $\mu$ s, Gain: 16.8dB .....37

14. Figure 14 Results from four zone PCB configuration (A) (B): 47498.609  $\mu$ s Gain: 12.8dB (C)(D) Exposure: 280081.130  $\mu$ s Gain: 2.4dB. the wrist's dorsal view was captured; however, the light is dispersed in the shot, indicating that it is not directly penetrating the tissue. stating the limitation in configuration 2.....38

15. Figure 15 Results of modified four zonal PCB configuration with (A) Exposure: 904.609  $\mu$ s gain: 11.8 dB (B) Exposure: 1528.870 Gain: 10.8 dB; Images captured with the camera hood and three sides dorsal, two side angles illumination with PCB wrist band form factor with photo booth for this configuration. ....40

16. Figure 16 IR images A-x belongs to Subject 1, and B-x belongs to subject 2, (A-1, B-1) - All LED zones on wristband turned ON, (A-2, B-2) - Only Center zone LEDs turned ON, (A-3, B-3) Only LEDs on either side turned ON, (A-4, B-4) LED's around the NIR camera turn.....41

17. Figure 17 Represents the sample1 of subject 1 for DoT results with four rows; each row represents values from each sensor converted through ADC to digital and taken as graphs. x-axis represents the number of samples taken for 30 seconds and y-axis represents the Voltage value converted. Samples taken when all the location LEDs turned ON (palmar,dorsal,sides) and all the 4 sensors capturing data on different locations of wrist.....43

18. Figure 18 Represents the sample 2 of subject 1 for DoT results with four rows; each row

represents values from each sensor converted through ADC to digital and taken as graphs. x-axis represents the number of samples taken for 30 seconds and y-axis represents the Voltage value converted. Samples taken when all the location LEDs turned ON( palmar,dorsal,sides) and all the 4 sensors capturing data on different locations of wrist.....43

19. Figure 19 Represents the sample 2 of subject 3 for DoT results with four rows; each row represents values from each sensor converted through ADC to digital and taken as graphs. x-axis represents the number of samples taken for 30 seconds and y-axis represents the Voltage value converted. Samples taken when all the location LEDs turned ON (illumination- palmar,dorsal,sides) and all the 4 sensors capturing data on different locations of wrist.....45

20. Figure 20 Represents the sample 1 of subject 3 for DoT results with four rows; each row represents values from each sensor converted through ADC to digital and taken as graphs. x-axis represents the number of samples taken for 30 seconds and y-axis represents the Voltage value converted. Samples taken when all the location LEDs turned ON (illumination- palmar,dorsal,sides) and all the 4 sensors capturing data on different locations of wrist.....45

## TABLES

Tables	Page
1. Table 1 IR spectrum with their corresponding wavelengths .....	2
2. Table 2: Conversion of Sensor output to voltage values- Table of Measurements and Calculated values .....	31
3. Table 3 MSE table showing similarity and dissimilarity between tables. ....	47

## ACKNOWLEDGEMENTS

I would like to express my sincere gratitude and appreciation to all those who have contributed to the completion of this thesis. Their support, guidance and encouragement were invaluable throughout this journey. Primarily, I am deeply grateful to my thesis advisor, Dr Rahman, for their unwavering guidance, expertise, and continuous support. Their insightful feedback, patience and dedication have been instrumental in shaping this research project. I would like to extend my gratitude to the members of this thesis committee, Dr. Preetham Goli, Dr. Mahbube Sidikki for their valuable time, expertise, and constructive feedback. Their valuable insights and suggestions have contributed to the overall quality and rigor of this thesis.

My heartfelt appreciation goes to my family and friends for their unwavering support, encouragement and understanding throughout my academic journey. Their love, motivation, and belief in me have been my driving force, and I am forever grateful for that. Presence in my life. Their support has made this research experience memorable and enjoyable. Lastly, I would like to acknowledge the participants who generously volunteered their time and participated in the data collection process. Their contribution is invaluable and has made this research possible. To everyone who has played a part, big or small, in the completion of this thesis, I extend my deepest gratitude. Your support and encouragement have been invaluable, and I am grateful for the opportunity to have worked on this research project. Thank you all.

## CHAPTER 1

### INTRODUCTION

A biometric system constitutes a technological approach that hinges on distinctive psychological or behavioral attributes of individuals to establish and authenticate their identity. The present study centers its attention on two specific biometric modalities: Diffuse Optical Tomography (DoT) and Vein Imaging Technique. In the context of Diffuse Optical Tomography (DoT), infrared (IR) Light-Emitting Diodes (LEDs) are employed for illumination, while IR sensors—typically photodiodes—are utilized to detect the interactions between IR light and biological tissues. In contrast, vein imaging leverages IR LEDs and an IR camera to capture vein patterns on the wrist. While vein imaging primarily gauges the propagation of light through tissues, DoT extends its purview by reconstructing internal tissue structures and functional parameters. The evolution of the IR imaging setup takes into account considerations such as light illumination, penetration depth, image quality, and ambient light control, resulting in multiple iterations of DoT systems based on principles of light propagation, data collection methods, consistent observations, sensor input, analog signal processing, and meaningful information extraction via the MSE technique. These methodologies empower DoT to visualize distinctive vascular response patterns within biological tissues, thus presenting promising potential as biometric identifiers.

Within the scope of this project, we harness lightweight wristband materials and optimize hardware design to minimize the overall weight of the system, thereby rendering it suitable for handheld or wearable deployment. This endeavor yields a handheld or wearable device characterized by compact dimensions, efficient light sources, streamlined circuitry, and reduced power demands from the Raspberry Pi, utilizing voltages up to 5V to facilitate low power consumption. This, in turn, extends operational durations without frequent recharging or power source replacement. This developmental stride yields a condensed, lightweight, and energy-efficient vein imaging system, potentially adaptable to integration within a wearable wristband form factor to cater to real-time biometric applications.

These hardware systems function on the principle of light penetration and absorption within biological tissues. Near-Infrared (NIR) light, spanning wavelengths from 700 to 1000 nanometers, boasts the distinct capability of deeper penetration compared to visible light, owing to diminished scattering and absorption by biological constituents. In this context, the wavelength employed is 870nm for the LEDs.

Presented below is a table illustrating the IR spectrum along with their corresponding wavelengths, although this framework exclusively employs Near Infrared wavelengths.

Table 1 IR spectrum with their corresponding wavelengths

<b>IR spectrum region</b>	<b>Wavelength range(nm)</b>
<b>Near infrared (NIR)</b>	700- 1400
<b>Shortwave infrared (SWIR)</b>	1400- 3000
<b>Mid- Wave Infrared (MWIR)</b>	3000-8000
<b>Long- Wave Infrared (LWIR)</b>	8000- 15,000
<b>Far infrared (FIR)</b>	15,000-1000000

Note. The table offers a comprehensive overview of the distinct divisions encompassing the infrared (IR) spectrum, along with their approximate wavelength intervals. Each of these divisions possesses its unique attributes and finds specific applications of particular significance is the near-infrared (IR) range, spanning from 700 to 1400 nanometers, which holds particular relevance for endeavors like vein imaging and optical tomography. These applications capitalize on near-infrared light for the purposes of functional imaging and physiological measurements.

## 1.1 Background

The origins of biometrics [\[1\]](#) can be traced back to ancient civilizations, wherein physical attributes such as fingerprints, facial features, and body measurements found application in identification endeavors [\[19\]](#). These methodologies predominantly relied on manual processes and lacked the technological sophistication witnessed in



contemporary biometric systems. Subsequently, during the 1960s, the advent of automated fingerprint identification systems (AFIS) brought about a transformative shift in biometric identification. This innovation harnessed digital imaging and pattern recognition algorithms [24] to enhance precision and efficiency. Biometric systems have since broadened their scope to encompass diverse modalities beyond fingerprints, incorporating elements like facial recognition, iris recognition, voice recognition, and other psychological and behavioral traits for biometric identification [2] and verification.

Historically, biometric systems necessitated intricate and cumbersome setups owing to the presence of multiple light sources, detectors, and associated electronics. However, ongoing technological progress has facilitated the miniaturization of components, facilitating the emergence of more compact DOT and vein imaging systems. The integration of optical imaging techniques into the realm of biometric systems signifies a notable advancement. Examples include facial recognition using visible light cameras or iris recognition employing infrared light, allowing for more precise and intricate capture of biometric characteristics.

DOT and vein imaging have arisen as specialized techniques within the domain of biometric systems. These techniques employ near-infrared light to analyze distinct optical attributes of biological tissues, encompassing parameters such as blood flow, oxygenation levels, and tissue perfusion. For instance, the wrist's vein patterns can be captured via an imaging system for authentication, while diffuse optical systems can assess oxygenation levels. This noninvasive methodology yields several advantages, including contactless accuracy, field-readiness, real-time imaging, and potential resilience against spoofing

attempts [\[27\]](#)[\[6\]](#).

An exploration of the literature pertaining to Diffuse Optical Tomography (DoT) reveals a notable absence of wearable DoT systems tailored specifically for the forearm or wrist, despite the existence of various DoT systems deployed in medical contexts [\[26\]](#) for functional imaging of tissues and organs. Many existing DoT systems are characterized by bulkiness and are ill-suited for continuous real-life monitoring. Additionally, investigations into vein imaging techniques have investigated both reflected and refracted light imaging for finger vein recognition, necessitating limited penetration of infrared light due to the shallow depth of finger veins. Consequently, the requisite illumination intensity for such applications is notably lower in comparison to traditional DoT systems designed for deeper tissue imaging. The survey of existing literature underscores the potential for crafting a groundbreaking wearable DoT system that captures functional data from the forearm or wrist. Such a system bridges the gap between conventional DoT setups and wearable biometric devices, enabling real-time monitoring and biometric recognition across diverse applications. This survey underscores the significance of accounting for the specific requisites and constraints associated with distinct imaging techniques when devising wearable systems tailored to specific anatomical regions.

## **1.2 Problem Statement**

Although research on Diffuse Optical Tomography (DoT) has been conducted, it is evident that a scarcity of wearable DoT systems tailored specifically for the forearm or

wrist persists, despite the existence of several DoT systems utilized in medical contexts for the purpose of functionally imaging tissues and organs. A majority of the existing DoT systems exhibit a substantial size and are not well-suited for continuous monitoring within real-world situations. Moreover, inquiries into vein imaging techniques [24] have explored both reflected and refracted light imaging for the recognition of finger veins [25], a process that necessitates limited penetration of infrared light due to the relatively shallow depth of finger veins. Consequently, the degree of illumination required for these applications is markedly lower in comparison to conventional DoT systems that are designed for the imaging of deeper layers of tissue.

The comprehensive review of existing literature underlines the potential for devising an innovative wearable DoT system, one with the capability to capture functional data from the forearm or wrist. Such a system would effectively bridge the existing divide between established DoT setups and wearable biometric devices, thereby facilitating real-time monitoring and biometric recognition across a diverse array of applications.

### **1.3 Objectives**

The objective is to develop a wearable biometric form factor for diffuse optical tomography and imaging techniques that combines the advantage of biometric technology with convenience and portability of a wearable device. Such a system would enable non-intrusive real time biometric data capture and analyze analysis in various applications including healthcare, sports, and personal authentication [26]. To fully answer the research question, the following objectives will be pursued:

- Build a compact, wristband form factor and 5V power requirement DOT system.
- Optimize the systems functionality including signal to noise ratio, resolution, accuracy, and insensitivity while adhering to the constraints of size, weight, and power.
- To assess the feasibility of forearm DoT as a biometric modality and demonstrate the utility of simultaneously capturing vein patterns from the same area.
- Conduct a comprehensive data collection and evaluation to assess the performance and effectiveness of proposed system or methodology.
- Analyze and evaluate the proposed framework's configurations results and acquire the best image quality for identification.

#### **1.4 Limitations**

Few limitations that are observed while researching as follows:

- During experiments involving IR imaging for wrist vein data collection [28], it is essential to consider certain factors to ensure accurate results.
  - One crucial consideration is to shave the tissue area of concentration, ensuring there is no hair present. Hair can interfere with the imaging process, potentially obscuring the vein patterns. And affecting the system's ability to accurately capture and analyze the vein data.
  - Additionally, individuals with tattooed areas should be avoided as the system make encounter difficulties distinguishing between. This texture

of the skin and highlighted tattoo leading to potential interpretation of vein patterns.

By taking this consideration into account, the reliability and accuracy of the wrist vein imaging system can be maximized during data collection.

## **1.5 Thesis Organization**

There are five separate chapters that make up this thesis. The first chapter serves as an introduction, laying the groundwork for the discussion that follows. The second chapter looks into hardware design and explains how wearable systems for diffuse optical tomography (DoT) and infrared imaging have evolved over time. The progression and integration of relevant elements are highlighted. The third chapter provides a thorough explanation of the test methodology and data gathering techniques. This chapter clarifies the methods used to obtain important data. The fourth chapter that follows provides an in-depth analysis of our work within a wider framework. This section conducts an analytical review of the results and consequences of our study. The fifth chapter, which summarizes the overall results, brings the thesis to a close. This chapter concludes with a brief overview and gives suggestions for possible directions for further study.

## CHAPTER 2

### HARDWARE DESIGN

The development of the succeeding configurations was the result of careful consideration of numerous aspects within a hardware engineering apparatus. Data analysis, signal duration, signal-to-noise ratio, and imaging depth were all carefully considered during this process [11]. These factors had a significant impact on how the design constructs were formed. Data analysis in particular played a crucial role since it had a significant influence on whether the collected picture could be used for vein pattern recognition analysis and the collection of diffuse optical tomography (DoT) data. As a result, the configurations were carefully planned to maximize data analysis capabilities, guaranteeing the clear and accurate extraction of vein patterns [20] from the captured images. A crucial aspect of the project was the effort to maximize the signal-to-noise ratio. Our goal was to improve the dependability and quality of the collected imagery by maximizing the signal and simultaneously eliminating unnecessary noise. In order to achieve this, the configurations were designed with a conscious focus on this goal, utilizing strategies such as careful calibration, ambient light regulation, and judicious exposure and gain setting adjustments. The accomplishment of an ideal signal-to-noise ratio was made possible by all these approaches taken in combination.

Furthermore, during the configurations' development, the aspect of imaging depth played a crucial role. Our goal was to increase the amount of infrared (IR) light that could penetrate human tissue by creating a change in the wavelength of the LED light source

from 940 nanometers to a strong 870 nanometers. In turn, this strategic change enabled enhanced imaging depth [11] and improved visual recognition of deeper vascular structures [20].

The configurations were carefully developed to comply with the requirements of hardware engineering by taking these factors into account and making the necessary adjustments. This thorough customization made sure that the highest levels of data analysis, signal-to-noise ratio, and imaging depth were achieved. The advancement of wrist imaging technology was greatly aided by these improvements, which were crucial in achieving accuracy and dependability in vein pattern recognition [17].

## **2.1 DOT Hardware design**

The latest advancement from vein imaging is diffuse optical tomography (DoT)[4]. Contrary to traditional imaging, which focuses on the measurement and examining of light propagation through tissues, DoT goes beyond this by reassembling images that show the intrinsic organization and functional characteristics of tissues [10],[9]. To produce three-dimensional maps showing the distribution of light absorption and scattering across the tissue, DoT really combines a variety of measurements and statistical methods. This methodology provides a thorough three-dimensional perspective [5] by facilitating the viewing and quantitative assessment of significant tissue properties, such as blood oxygenation, blood flow [12], and the concentration of particular chromophores. When compared to traditional imaging approaches, DoT's implementation increases spatial resolution [11], providing enhanced structural and functional data. As a result, it makes it

possible to evaluate tissue structure more accurately, spot functional changes, and gain a better understanding of tissue physiology.

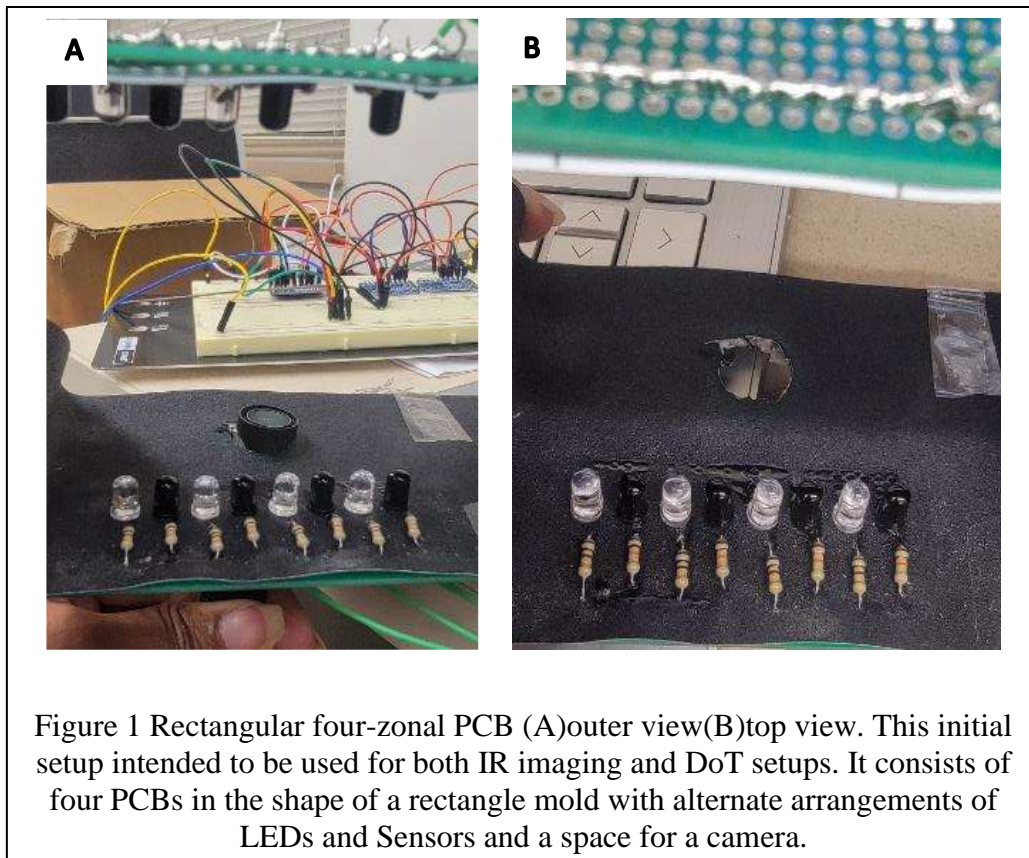
Infrared (IR) LEDs, sensors, and an Analog-to-Digital Converter (ADC) are essential elements of a DoT system. The ADC is used to convert sensor data into digital representation. The system's microcontroller, a Raspberry Pi, manages human interaction and graphically displays digital data on a monitor. The system's components are likewise powered by this set-up, up to 5V. Infrared light from the IR LED is emitted into the biological tissue at its point where it interacts with the medium and functions as an illumination source. Light interacts with the tissue in this way in which some of it is absorbed and the rest scatters or passes through the tissue. The IR light that has passed through the tissue or that has been reflected back toward its surface is picked up by a sensor, usually a photodiode. The DoT system determines the fundamental optical characteristics of the tissue by measuring the light intensity at various geographical positions, assisted by mathematical algorithms. This leads to the creation of a collection of functional and physiological insights, including information on things like tissue perfusion, oxygenation [\[6\]](#) levels, and blood flow.

### 2.1.1 Experiment 1: Rectangular Four-zonal PCB setup

The initial DOT setup, which included a unique arrangement of LEDs and sensors, was created to accommodate both IR imaging and the dot system. This method involved placing a specific LED next to each sensor on each PCB, defining distinct regions known as top-bottom-side zones that corresponded to various PCBs with identical LED and sensor arrangements. In



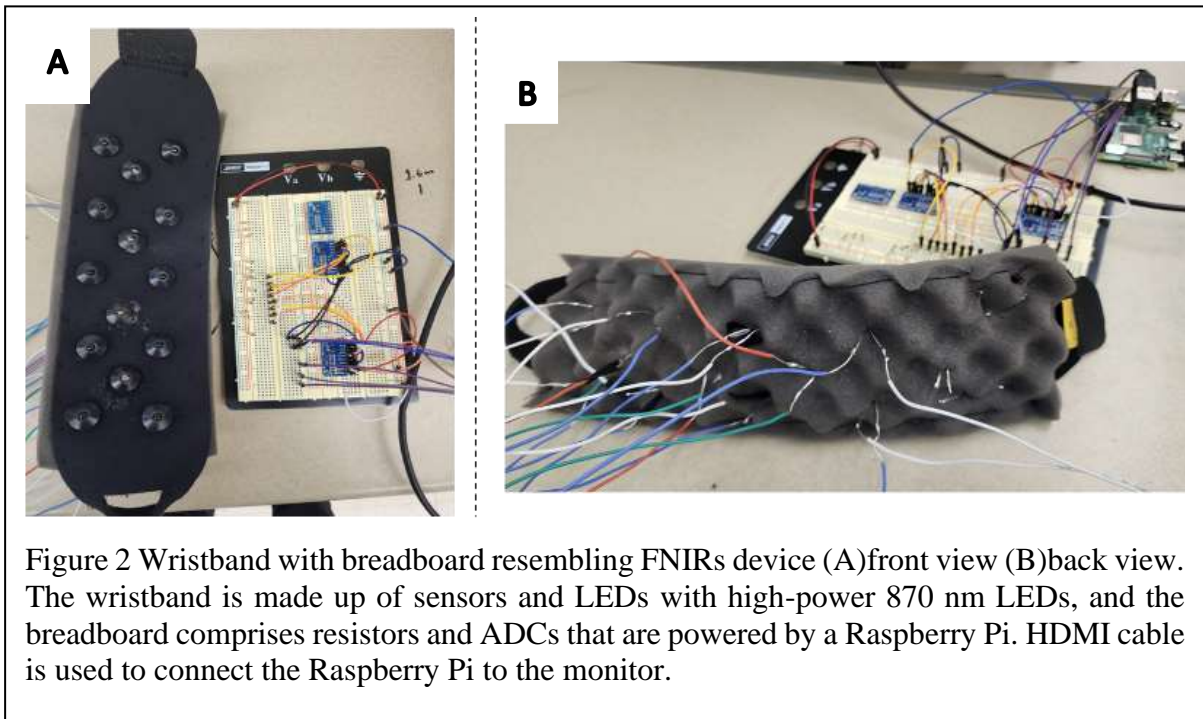
this configuration (figure 1), sensors with a wavelength of 940 nanometers were used in addition to LED modules with that wavelength. Unfortunately, this specific arrangement was unable to produce the anticipated amount of illumination needed for accurate data collection and appropriate imaging.



### 2.1.2 Experiment 2: wrist band Form resembling an FNIR.

We initiated a series of studies in our lab using the Functional Near Infrared Spectroscopy (FNIRS) equipment to collect data. The idea behind FNIR, a functional imaging technology used to track brain activity, is that changes in neural activity correspond to changes in local cerebral blood flow and oxygenation. We decided to

recreate the setup inherent to FNIRs [10] using a cheap wristband purchased from a nearby pharmacy [15] in order to create a cost-effective framework [23]. Significant changes were made to this innovative arrangement, most notably replacing the old 940 nm LEDs with stronger, more potent 870 nm LED units. A set of four proximally positioned LEDs encircled each sensor. LEDs and sensors were the only components that could fit on the wristband; the Analog-to-Digital Converter (ADC) and resistors were interfaced with the breadboard during the initial stages of research. The Raspberry Pi microcontroller's 5 Volt supply served as the source of power for the entire assembly. To effectively control ambient light, the LEDs and sensors underwent a procedure that involved painting them with black nail polish and using black diffusers as shown in figure 2.



### 2.1.3 Experiment 3: wrist band with PCB board

A significant improvement was made by moving all components from the breadboard to a printed circuit board (PCB) in response to the wiring issues seen in the previous setup. The resistors and Analog-to-Digital Converters (ADCs) were among the components on this newly designed PCB that underwent direct soldering onto the substrate, resulting in a layout that was more compact and effective. This change had two positive effects: it reduced the possibility of loose connections and significantly improved the configuration's overall stability and dependability. The adoption of the new PCB shown in figure 3, represented the start of increased organization and streamlined setup, assuring the steady flow of data collection while also minimizing the possibility of any plausible disturbances during research.

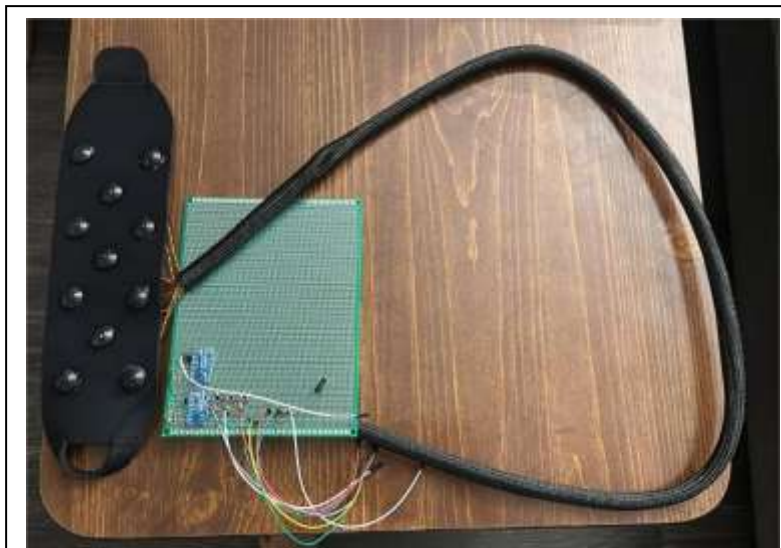
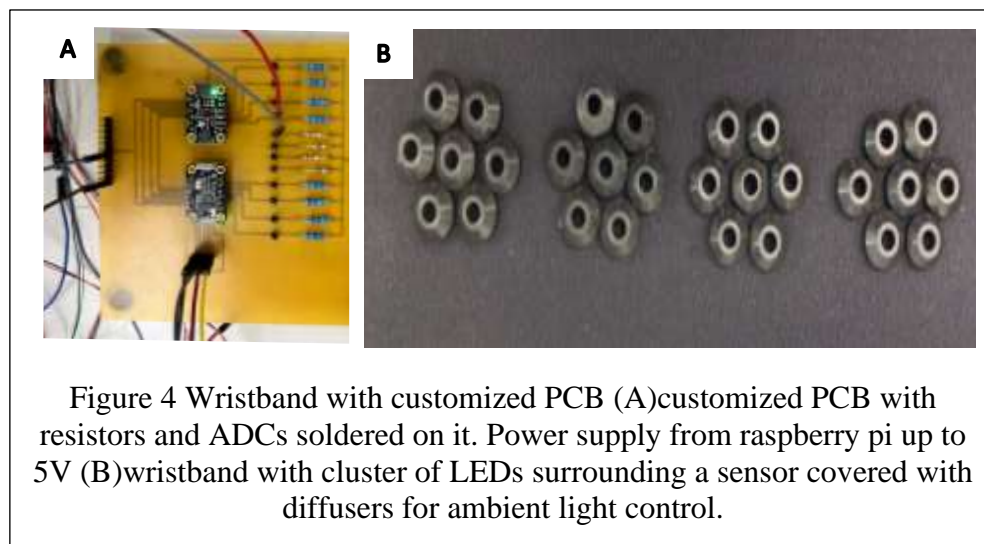


**Figure 3 wristband with PCB**  
Wristband with PCB to reduce the wiring and avoid loose connection. Resistors and ADCs soldered on PCB. Power from raspberry pi.

#### 2.1.4 Experiment 4: wristband with customized PCB

We developed a customized printed circuit board (PCB) to address issues with soldering, such as excessive lead application and the presence of gaps in the soldering locations within the earlier circuitry. The installation of connections now has a higher level of precision and reliability thanks to this custom PCB design. A careful and effective component integration was accomplished using the customized PCB, minimizing any potential soldering-related issues. Additionally, by placing clusters of LEDs next to each sensor, we increased the brightness of the light emitted by the LEDs around each one of the sensors. This strategic improvement was crucial in improving the precision and effectiveness of our wristband configuration, which was designed for data collection. In the framework of our experimental efforts, the integration of the customized PCB along with the increased LED luminosity collectively enhanced the system's overall performance and robustness, setup is shown in below figure 4.



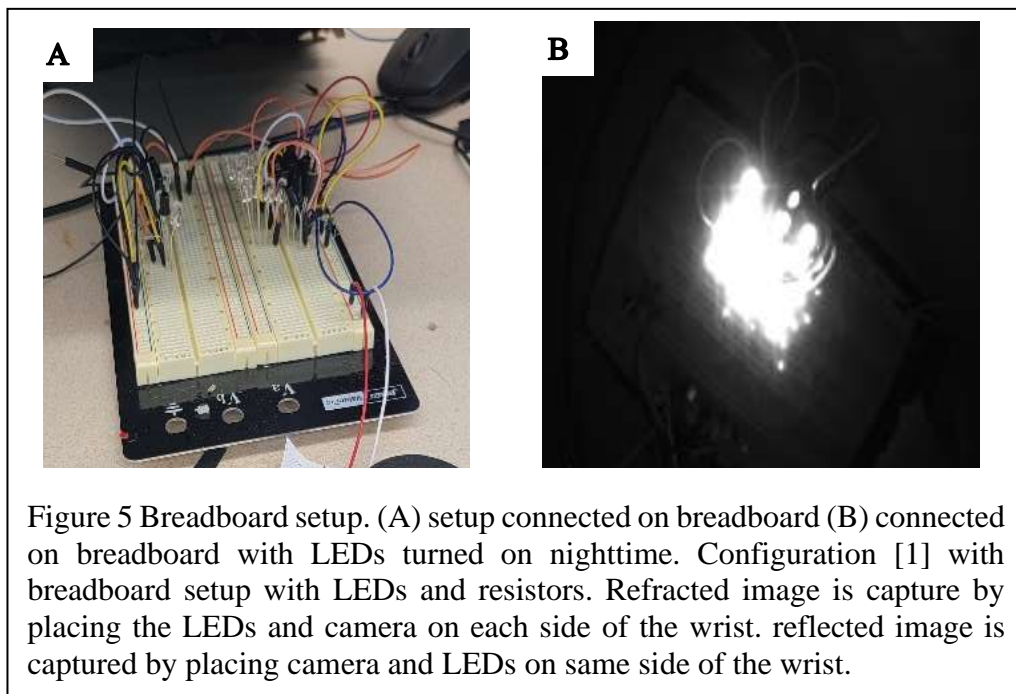
## 2.2 Vein Imaging System

Near-infrared light, or NIR light, is used in infrared (IR) imaging. The IR setup uses IR LEDs of the MTE8760N5 model, with a maximum power rating of 180mW and a working wavelength of 870nm. In addition to the camera hood, which is positioned 5 cm above the palmar side of the hand, the Alvium 1800 U-501 NIR camera [\[6\]](#) is a crucial element. Vein visualization and the gathering of physiological data are made easier by this systematic experimental approach. Such visualization is then explored for a variety of purposes, such as biometric identification, medical diagnostics, and the investigation of physiological processes. The Vimba software is used on a Windows PC to capture and process images that are taken through this technique.

NIR light is the primary source used by IR imaging to make veins visible and gather physiological data. The light sources used in this procedure are NIR LEDs, which are created to generate light at a certain wavelength, usually at 870 nm. These LEDs produce NIR light, which penetrates the body's targeted tissue or area. The lower wrist region of the arm is what is most important in this circumstance. A significant portion of the IR light is absorbed by veins because they contain deoxygenated hemoglobin and have a greater light absorption coefficient in the NIR region. The specialized NIR camera, designed to detect IR light, captures both transmitted and reflected light coming from the tissue.

### 2.2.1 Configuration 1: Breadboard Configuration

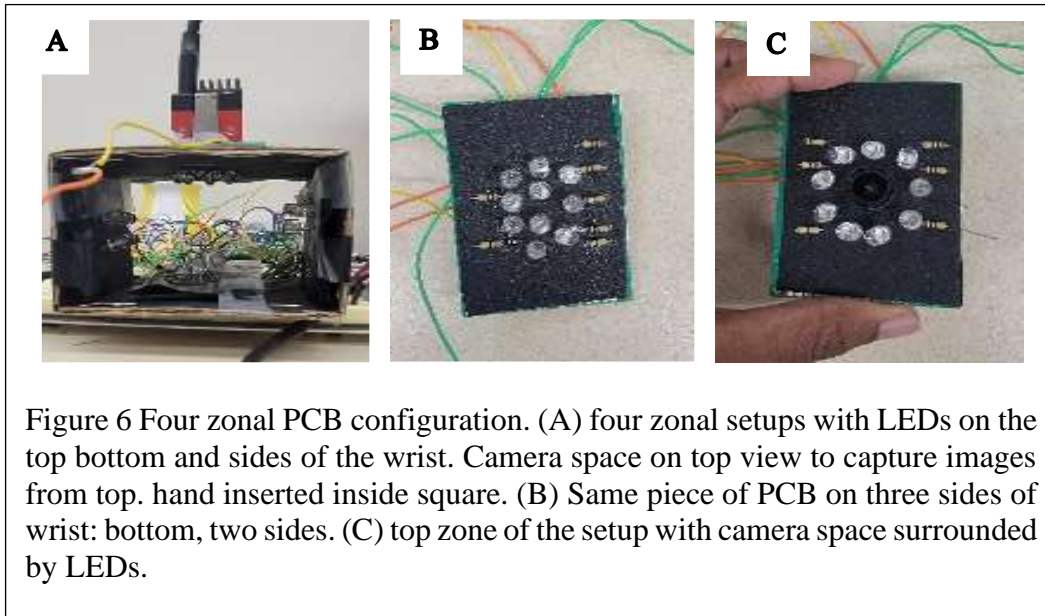
In the initial configuration, referred to as the Breadboard Configuration (figure 5), the IR LEDs were connected to resistors on a breadboard, and pictures of the palmar side of the wrist were taken in environments with natural daylight illumination. surprisingly, the veins remained visible in the photos even though there were no methods for controlling ambient light. The choice was made to capture vein photos at night because of the potential impact of ambient light on the quality of the images. The impact of ambient light was reduced as a result of this strategic change, which also increased the vein patterns' visibility and clarity in the captured images. Below is a diagram that serves as a reference for Configuration 1.



### 2.2.2 Configuration 2: Four-zone PCB Configuration

Due to its dependence on the indirect absorption of IR light into the tissue and inability to control ambient light, Configuration 1 has limitations. Only the palmar or dorsal side of the wrist received illumination, specifically [18]. Recognizing the necessity for increased light intensity and thorough coverage at the same time, we created a revolutionary configuration (refer figure 6) that consists of multiple zones, each with its own printed circuit board (PCB). The dorsal, palmar, and lateral angles of the wrist were all represented by different zones within each of these zones.

The PCBs were designed for direct skin contact to provide the best light transmission. The LEDs were coated with applied nail polish to increase light penetration even more. This allowed the LEDs to only stem light from their tips, which interacted with the tissue directly. We were able to capture vein patterns with greater clarity and detailed detail thanks to the careful alignment of the PCB layout with the skin's surface. Four zones and PCBs were integrated into the advanced configuration, which successfully overcame the drawbacks of Configuration 1 and improved upon them. By virtue of this improvement, greater control over ambient light, increased light intensity coming from all four aspects of the wrist, and improved direct tissue illumination were all made possible. These innovative steps played a crucial part in improving the accuracy and dependability of wrist vein imaging. For visual reference, Configuration 2 is shown in the following graph.

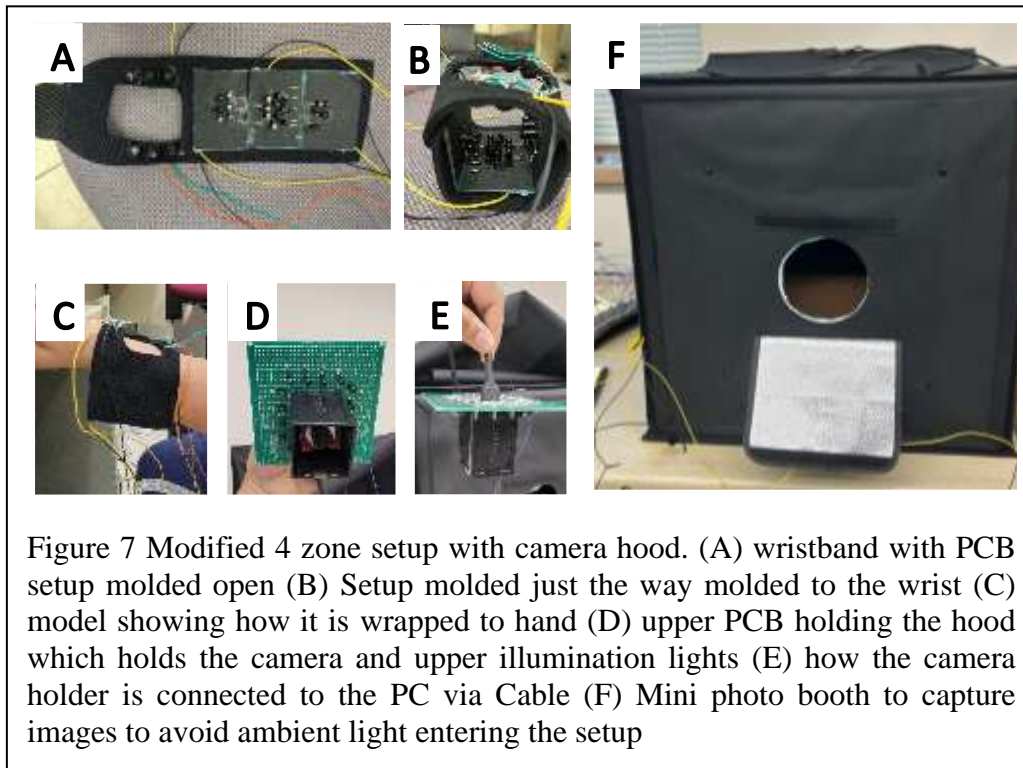


### 2.2.3 Modified Four-zone wristband Configuration with camera hood.

The previously mentioned four-zone PCB arrangement had the drawback of requiring four different PCBs, each of which included soldered LEDs. A strategically positioned camera opening on the topmost PCB allowed for the capturing of top-view photos. Even though this configuration was a significant improvement, our major goal was to create a setup that had a wristband-like form factor. To achieve this goal, a reasonably priced wristband was purchased from a nearby pharmacy [\[14,21,22,23\]](#). The dorsal and lateral angles of the wrist were then precisely captured by attaching the PCBs to three sides of the wristband. A significant barrier was also presented by the only reliance on nighttime image capturing. We decided to incorporate a mini-Photo Booth to deal with the impact of ambient light to get around these restrictions and guarantee consistent lighting conditions while taking pictures.



The wristband had a customized space at its upper portion to allow the camera and was tightly fastened around the wrist after being put in place. A restored toybox was cleverly used to function as a camera holder, specifically created to fit into the allotted space, to permit this creative configuration. It is important to draw attention to the configuration's three different zones of lighting, which stand for the wrist's dorsal [\[21\]](#) and two lateral angles. However, there was originally a lack of illumination in the fourth zone, which corresponds to the area around the gap designated for the camera holder. To overcome this obstacle, holes were added to the wristband in the area designated for the camera holder as a flexible modification. Using a glue gun, LEDs were carefully attached to this spot on the wristband. The implementation of this update successfully added illumination to each of the wristband setup's four zones. This final improvement, designated configuration 3(refer figure 7), represented the merging of the portability and simplicity indicated by a wristband with the features inherent to a PCB layout. The result was an efficient and practical resolution that made it possible to record vein patterns and plan wrist imaging tests.



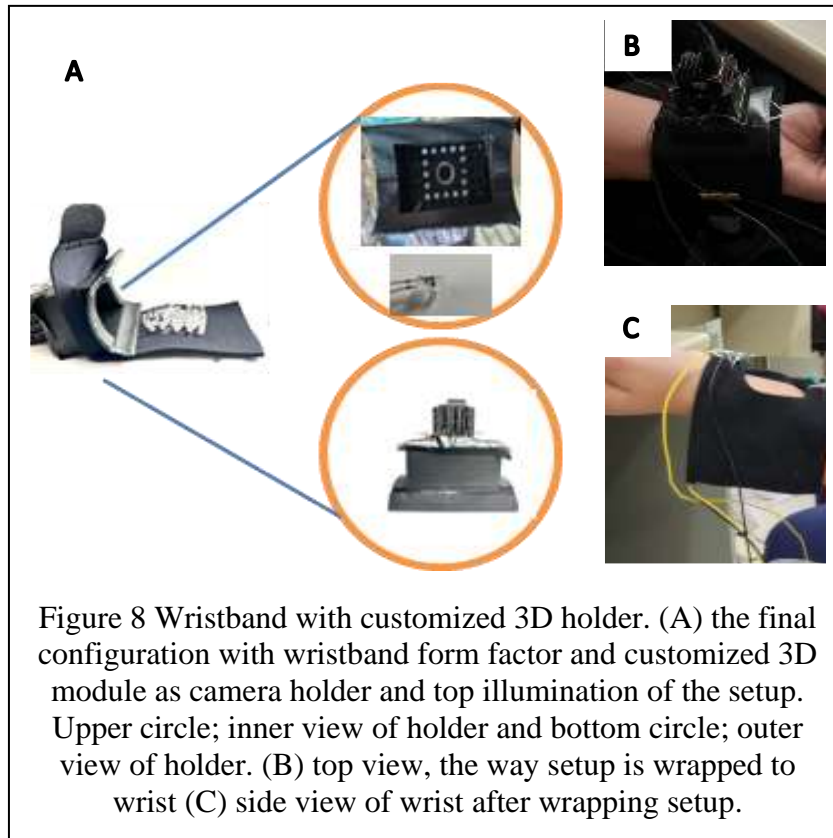
#### 2.2.4 Configuration 4: Enhanced illuminated wristband configuration with custom 3D Camera holder.

The development of a comprehensive wristband form factor that eliminated the need for different PCBs was the overriding goal that served as the basis for Configuration 3. During the experiment, a finding emerged: while the light was adequate for reflecting images, it was insufficient for refracting images. A parallel strategy was used in response, that involves the insertion of wristband holes for LEDs covered with black colored nail polish. By taking this calculated exposure, it was made sure that only the LEDs' outermost portions were directly illuminating the tissue on the wrist's three faces.

However, there was still reason for concern over the fourth illumination zone, which was close to the camera holder and was thought to be crucial for the recording of reflected

images. A customized 3D camera holder was used to overcome this obstacle. This holder included a defined space for the insertion of a group containing 16 LEDs, ensuring an adequate level of illumination for the proposed setup in addition to providing a secure location for the camera. The LEDs made direct contact with the tissue, which reduced the effect of ambient light and eliminated the need for a mini-Photo Booth as seen in Configuration 3, leading to the effective convergence of needs. Additionally, this design achieved the desired wristband shape while providing sufficient illumination for the capture of both reflected and refracted images.

The wristband configuration became an effective response to the difficulties encountered in earlier configurations by incorporating these strategic changes. As a result, it was possible to achieve enhanced illuminating capabilities, higher image quality, and a wearable structure that was practical for capturing vein patterns in both reflected and refracted light. The concluding image shows Configuration 4 in its final form (refer figure 8).

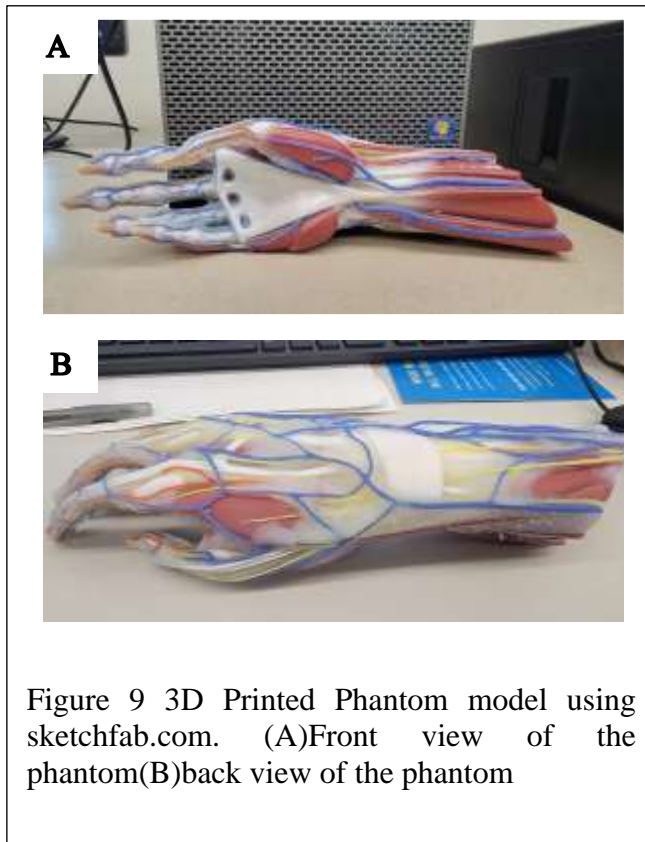


CHAPTER 3  
TEST METHODOLOGY

**3.1 IR Imaging**

We used a phantom model that resembled a human hand in the setting of our experimental framework, which was helpful for our vein imaging efforts. Using an existing hand model provided on Sketchfab.com, this 3D-printed phantom model was created. The incorporation of this phantom model (refer figure 9) provided a platform for cautious calibrations and preliminary evaluations, ensuring the highest level of accuracy and performance [11]. Before beginning to acquire IR images of human wrists, this phase of preparation was essential. The phantom model expertly captured the key characteristics of a human hand, providing a controlled and repeatable environment for our research projects.

After the phantom model's infrared images were successfully captured, our research was expanded to include human wrists. This growth made it possible to test the effectiveness of our wristband setup in current world circumstances. The image below illustrates the crucial function the phantom model played in our research and represents an important development in the steady advancement of our IR imaging technology.



### Light Source Positioning

Multiple light illumination configurations for vein imaging are shown within this framework, divided into two main categories: light transmission and reflected light. The positioning of the image sensor (NIR Camera), the wrist under inspection(refer figure 10), and the precise arrangement of LEDs are all included in these parameters. The methodical arrangement of LEDs is carefully organized to support the accurate and effective measurement of light's complex interaction with the tissue in both the light transmission and reflected light paradigms. This strategic design serves as a stimulant for the collection of valuable data essential for the study of physiological processes and functional imaging.

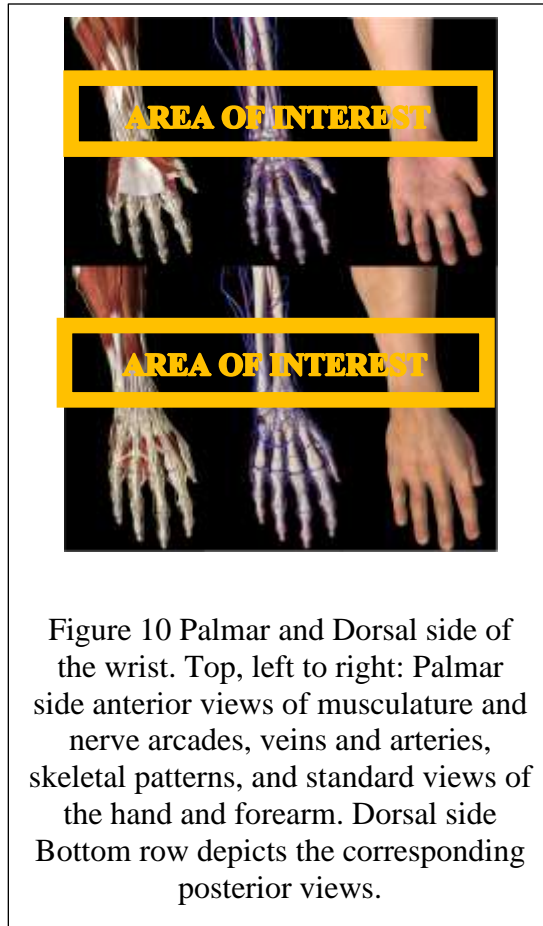


Figure 10 Palmar and Dorsal side of the wrist. Top, left to right: Palmar side anterior views of musculature and nerve arcades, veins and arteries, skeletal patterns, and standard views of the hand and forearm. Dorsal side Bottom row depicts the corresponding posterior views.

Light transmission and illumination position:

The precise positioning of light source to enhance light transmission is an essential component of the imaging setup. A common approach involves placing the light source on just one side of the wrist or tissue being observed in order to facilitate light transmission. The near-infrared (NIR) light that is emitted under this construction assumes penetration into the tissue, resulting in interactions with the underlying blood vessels and other essential aspects. By simply arranging LEDs with respect to the position of NIR camera and wrist, this approach creates a path for NIR light to penetrate through tissue,

allowing for the measurement of relevant light absorption and scattering properties.

The NIR camera's ability to record the transmitted light on the tissue's opposite side allows for eventual uncovering of a wealth of data about the captured tissue.

Reflected light and illumination position:

A key factor in achieving accuracy in results when using the reflected light methodology is how well the light source is positioned in relation to the wrist. The light source typically finds placement parallel to the NIR camera in this configurational framework. These LEDs' primary purpose is to emit near infrared light, which in turn illuminates the tissue or the specified region of interest. This light is emitted, and as it travels through the tissue, it experiences scattering and reflection phenomena [\[29\]](#). The NIR camera, which is positioned close to the LEDs, has the responsibility of capturing the light that reflects reflection. This reflected light contains plenty of essential data about the tissue's natural absorption and scattering properties. The system successfully carries out the capture and subsequent analysis of the reflected light by the careful arrangement of the positioning of both IR light source and the NIR camera(refer figure 11). This carefully planned interface supports the procedure of data extraction, giving the research project the capacity to extract crucial functional and physiological insights.



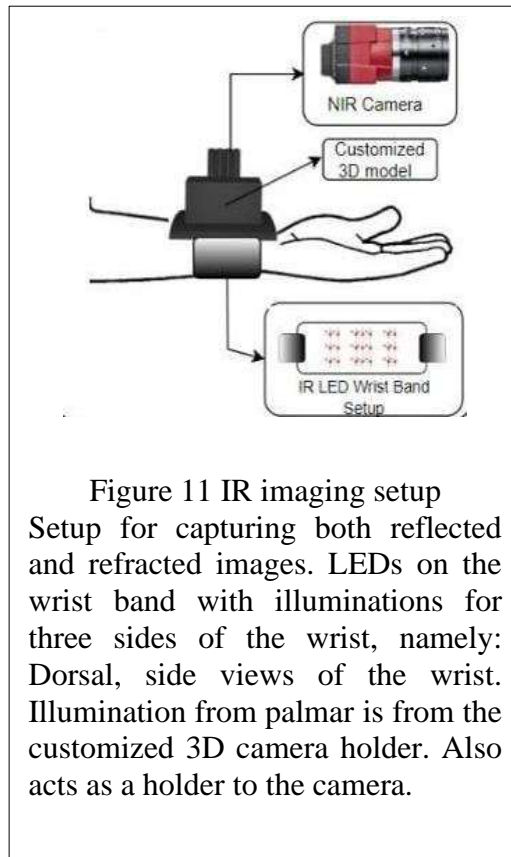


Figure 11 IR imaging setup  
 Setup for capturing both reflected and refracted images. LEDs on the wrist band with illuminations for three sides of the wrist, namely: Dorsal, side views of the wrist. Illumination from palmar is from the customized 3D camera holder. Also acts as a holder to the camera.

### Vimba as a software tool:

Within this framework, the most important Vimba software stands out as a crucial tool used for the capture of IR images. In addition to providing a user-friendly interface, Allied Vision's extensive software development kit (SDK), Vimba, also includes sophisticated control features specifically designed for industrial cameras. By utilizing Vimba's abilities, we were able to establish connections and communication channels with our IR camera with ease. This made it possible for us to quickly obtain high-quality IR images, which served as the foundation for our experimental efforts and subsequent studies. With Vimba, we had the power to adjust a variety of camera settings, including

the gain, white balance, and exposure duration. By adjusting these variables, we could coordinate image acquisition and get our desired results. Utilizing the Vimba software's capabilities, we improved our ability to gain insight into our database of acquired IR images, leading to the extraction of insights crucial to the success of our efforts in the field of infrared imaging.

The modification of exposure settings is a crucial component of our manipulation. The amount of time the camera's sensor is exposed to light while taking a picture is controlled by this software integration. Increasing the exposure duration results in the creation of brighter images, while decreasing it results in the creation of darker counterparts. In order to maximize the visibility of vein patterns and other minute details woven into the content of the infrared images being captured, this calibration acquires crucial importance.

Similar to this, the use of gain settings is supported by Vimba software. The signal from the sensor is amplified according to the gain setting. Raising the gain improves the image's luminance and contrast, improving visibility in dimly lit areas. However, it is crucial to use caution while manipulating gain because too much amplification can bring on noise and cause an image quality decline. A careful balance is essential when coordinating the interaction of exposure and gain settings to produce the best possible image quality. Here, increasing exposure can effectively address situations with dim lighting, while gain modulation comes into play to promote improved visibility. To avoid the effects of overexposure and excessive gain amplification, which can ruin the image's elegance by causing loss of clarity, making images faded, or causing increased noise levels, a word of warning is recommended.

We design a precision-infused image capture procedure by carefully adjusting the exposure and gain settings inside the Vimba software ambit. This calibrated setting guarantees that the IR images' delicate balance of brightness, contrast, and fine detail is maintained. This combination results in the accurate vein pattern recognition and analysis needed to give wrist imaging applications increased effectiveness and unwavering dependability.

### **3.2 DoT setup**

Infrared light emitting diodes (IR LEDs) like the MTE8760N5 model work with infrared sensors, usually photodiodes like the 100F5T-IR-JS-940NM version, to perform diffuse optical tomography (DoT). The delicate relationship between light and biological tissues is captured and studied in this synergy, with a focus on determining the blood's oxygen saturation levels. The selected region of interest, which is located in the lower wrist, is illuminated by the near-infrared LEDs after they have been carefully positioned. As it comes into contact with the blood vessels embedded inside the tissue, the produced near-infrared light takes on a characteristic path and interacts differently with oxygenated and deoxygenated blood. A result of this interaction is that oxygenated blood has a preference for absorbing near-infrared light, whereas deoxygenated blood excels in scattering and reflecting light. Infrared sensors and photodiodes are placed strategically to record these subtleties as the light impact change between reflection and transmission. After interacting with the vascular terrain and its environs, these sensors coordinate the measuring of light intensity.

The output from the infrared sensors emerges into an analog signal, requiring a changeover to the digital domain for further processing. Adafruit's ADS1115 Analog to Digital Converter (ADC) takes control for this crucial conversion. The ADC is tasked with converting analog signals from the sensors into their digital equivalents, where these digitized values serve as stand-ins for the light intensity sensed by the sensor following tissue involvement. These numerical interpretations reflect the amount of near-infrared light that the vascular network either absorbs or disperses, a feature organically linked to the current oxygenation levels in the flowing blood.

The results of this analytical process are materialized in Table 2 below, which includes the ADC data together with their transformed voltage analogs. A precise mathematical formulation must be used to convert the discrete analog to digital converter (ADC) results into a coherent voltage matrix. Below is a brief explanation of this formula, which is essential to the conversion process.

$$\text{Voltage} = \frac{\text{ADC Reading} * \text{Full Scale Voltage}}{2^{16} * \text{PGA}}$$

where the digital measurement collected from the ADC is represented by the ADC reading. Due to the fact that the ADC being used here has a 16-bit resolution and that n stands for the n bit resolution,  $2^{16}$  is represented as  $2^n$ . The Raspberry Pi delivers a voltage to the ADC or setup that is known as the full-scale voltage. The value of the programmable gain amplifier, or PGA, is set during data gathering when programming [28].

Table 2: Conversion of Sensor output to voltage values- Table of Measurements and Calculated values

<b>ADC OUTPUT</b>	<b>VOLTAGE CONVERTED (V)</b>
<b>563</b>	0.042953
<b>562</b>	0.042877
<b>563</b>	0.042953
<b>564</b>	0.04303
<b>564</b>	0.04303

The following figure 12 visually explains the method of the Diffuse Optical Tomography (DoT) tests. The wrist was completely encircled as part of the experimental framework, which resulted in the conduct of several trials. In these tests, the wrist's LED places were selectively lit while each sensor's response was carefully monitored. The method of operation involved deliberately disconnecting the other LEDs from the circuit while activating various LED combinations, including single LED activation, dual LED illumination, and the participation of three LEDs. We conducted a thorough investigation of the consequences experienced by the system's performance in light of various LED configurations by closely examining the sensor-generated data. The current section provides an overview of the data stores collected while presenting examples of these analytical studies.

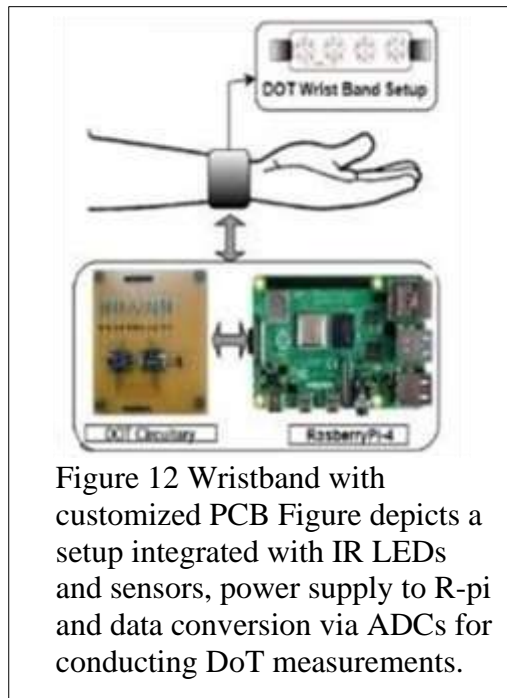


Figure 12 Wristband with customized PCB Figure depicts a setup integrated with IR LEDs and sensors, power supply to R-pi and data conversion via ADCs for conducting DoT measurements.

### User Instructions:

The provision of clear instructions to the user becomes essential prior to the start of the acquisition of Infrared (IR) images and Diffuse Optical Tomography (DoT) data covering both the reflector and refractor perspectives. Such instructions form the basis of a methodical experimental path, which is characterized by carefully controlled ambient lighting and the thorough execution of calibration procedures. The instructions that must be conveyed to the user in the next explication are summarized.

First and foremost, it is the user's responsibility for encouraging cooperation throughout the image capture process. The learning of appropriate posture and deft hand movement control become of utmost importance [14]. The user must be made aware of the necessity of maintaining a constant wrist posture and the attentive maintenance of a

constant distance between the wrist and the camera, creating a solid basis for the capture of images of the highest possible quality. In order to properly align the user's wrist before beginning the imaging procedure, the user must receive detailed instructions. Depending on the selected viewpoint, the alignment principles in vein imaging vary. Either the dorsal or palmar aspect must be angled for the reflected view. If a custom three-dimensional holder is used, a crucial restriction enters the picture. In these situations, the user must get careful instruction on how to align and position their wrist securely within the boundaries of the holder. These speeds up a seamless fusion of accurate alignment and unshakeable stability, both of which are essential for the imaging job.

The iterative process of image collection draws the user's attention and calls for keen observation of a number of factors. These include making sure the appropriate focus is attained, carefully framing the scene, and carefully adjusting the exposure settings. In order to ensure a thorough capture of both the wrist and the delicate patterns of veins, the user must be inspired to begin the capture of a series of images using a planned move designed to take in a range of angles and aspects. The serious goal of exposing the anatomical landscape of the wrist from many angles underpins the pursuit of these different images. Before beginning the image capturing job, a calibration ritual must be carefully carried out to add another level of care. To reduce the detrimental effects of background noise or the vagaries of changing lighting conditions, this calibrated beginning comprises the gathering of reference images clear of any wrist or vein present.

## CHAPTER 4

### RESULTS AND DISCUSSION

The results of experiments and discussions that followed have highlighted the fact of certain restrictions in each configuration. When these limitations were acknowledged, it became clear that the setup needed to be improved and advanced. The planning of succeeding configurations has been greatly aided by the function of these limitations as instructive signposts. We identified specific domains in need of careful attention and improvement by carefully examining the results provided by each trial. This assessment covered a range of restrictions, including those related to ambient light control, image detail, illumination uniformity, and the overall system performance. Equipped with these insights, we set out to create an innovative setup that was carefully designed to address the limits that had been identified. The gradual progress made to improve the system's efficacy and robustness has been made possible by the iterative rhythm of this developmental action. Each new arrangement represents a step forward and a leap above previously revealed limitation. This allowed for the seamless integration of creative techniques and innovative components, each of which served as a tactical weapon in the larger effort to optimize various aspects of the setup.

We have gathered a wealth of invaluable information by having thorough discussions about the experimental results and careful evaluations of the constraints discovered. This abundance of data served as the favorable ground from which further

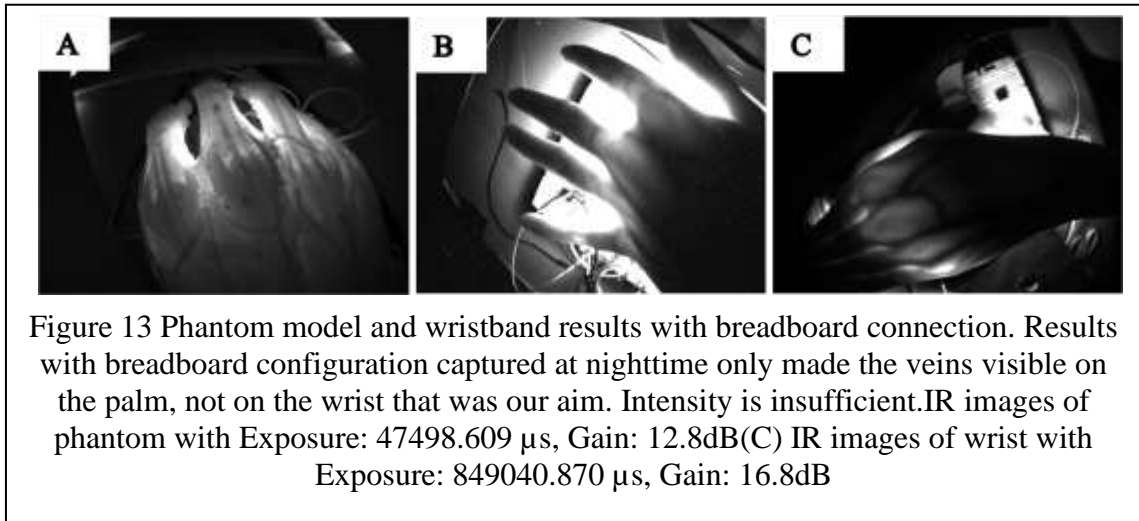


developments in the field of study sprouted. An everlasting patchwork of improvement has emerged from the iterative rhythm, which includes the process of constraint exploration, the development of new configurations, and the ongoing improvement of the setup. The result of this planned evolution has been a continuous improvement in the system's effectiveness, reliability, and precision in the admirable goal for imaging excellence.

#### **4.1 IR Imaging**

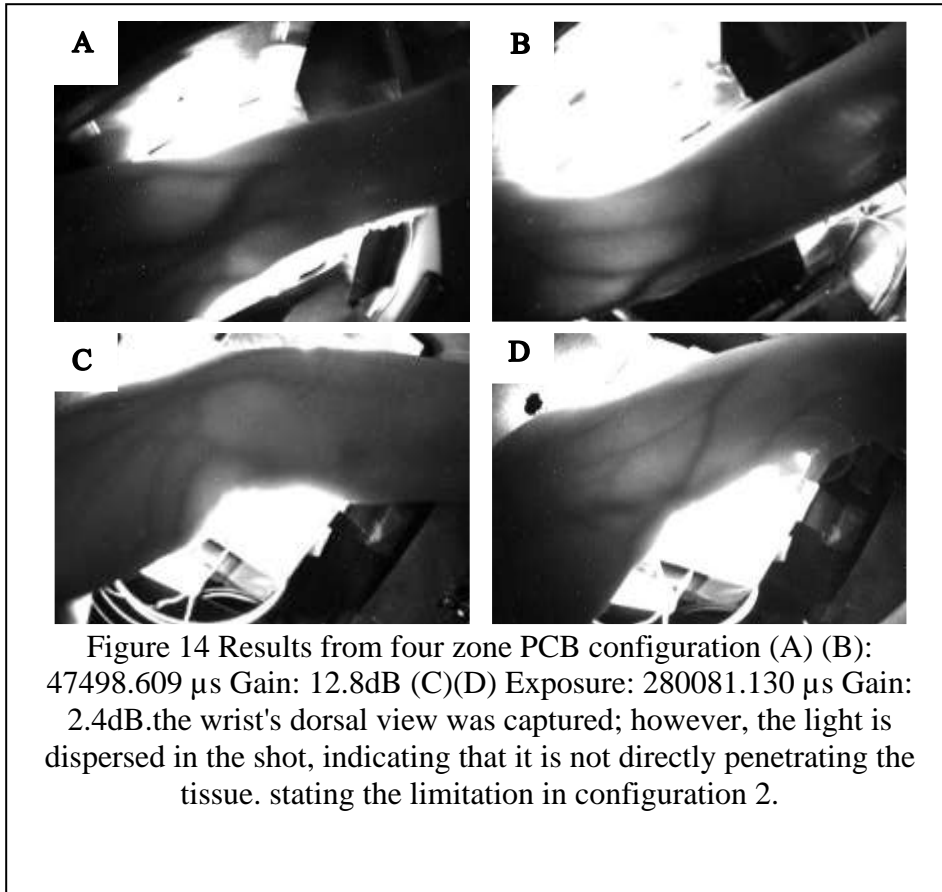
Experiment - 1: Breadboard configuration.

The results of the initial design(refer figure 13 below), which used a breadboard connection, have shown a number of restrictions. The photos obtained with this configuration are affected by uncontrolled ambient light, and they could only be taken at night to reduce the presence of extraneous luminance. This setup's limited scope has had an impact on both its practical usefulness and adaptability. The obvious lack of mechanisms for ambient light adjustment, a gap that has dampened the quality and trustworthiness of the acquired images, was one important finding from this approach. This has furthered the need for future configurations to introduce improvements that can get around this current limitation.



#### Experiment - 2: Four zone PCB configuration.

The results of the second configuration (refer figure 14 below) have shown limits. Despite having four different zones to cover both the palmar and dorsal faces of the wrist, this design was limited to only illuminating one of them at any given time. This restriction limited the ability to take pictures that could fully display both the wrist veins as they are refracted and as they are reflected. Furthermore, the light intensity was found to be insufficient to capture complex and clear refracted images, lowering the accuracy of the images that were acquired. It was still plagued by difficulties in achieving ideal illumination and simultaneously recording refracted and reflected viewpoints. These discoveries have highlighted the necessity for more improvements and developments in succeeding configurations to get over these constraints and increase the effectiveness of wrist vein imaging.



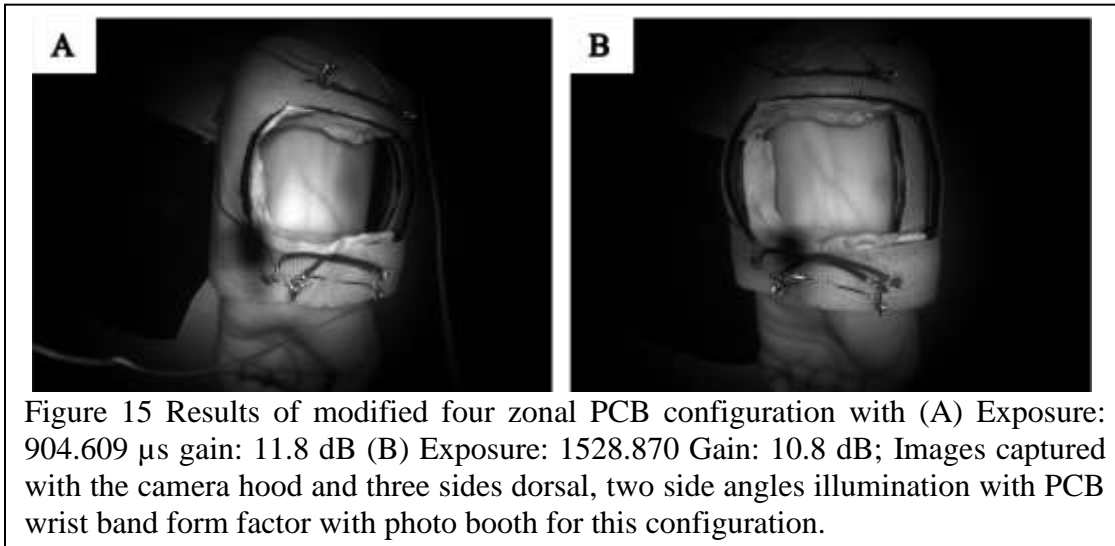
### Experiment - 3: Modified four zone wrist band configurations with camera hood.

Certain restrictions have been revealed by the third configuration's findings. Despite having been designed to address several shortcomings of the previous setup, this configuration had a number of drawbacks of its own. The dorsal side and two side angles of the wrist were the only three facets of the wrist that were illuminated by this configuration. Unfortunately, the palmar side of the wrist was not addressed, which is equally important for recording vein patterns. Additionally, there was a space that needed to be filled for the camera to take pictures. As a result, a camera hood was developed to act as a camera holder. Additionally, the use of PCBs in this layout created tiny gaps that

unintentionally allowed ambient light to enter, thereby lowering the quality of the images that were collected. Additionally, the addition of PCBs made it more difficult to fully realize the sought wristband form factor because the system still included separate parts that weren't perfectly merged into one another. The need to overcome the limitations seen in the second configuration sparked the evolution of this configuration. It aimed to achieve the wristband shape while guaranteeing direct LED light output onto the tissue to improve illumination. This goal was achieved by strategically exposing LED tips, with the rest of the LED surface coated in black nail paint.

This modification made it easier to precisely target the light onto the wrist, which lessened the restriction of indirect illumination seen in the previous configuration. Despite its shortcomings, this evolutionary design is a significant step forward and lays the foundation for further improvements and revisions. With the overriding goal of attaining a wristband-based form factor and enhancing lighting to completely capture vein patterns, the insights gained from the third configuration have provided the groundwork for the development of more refined and optimal settings.

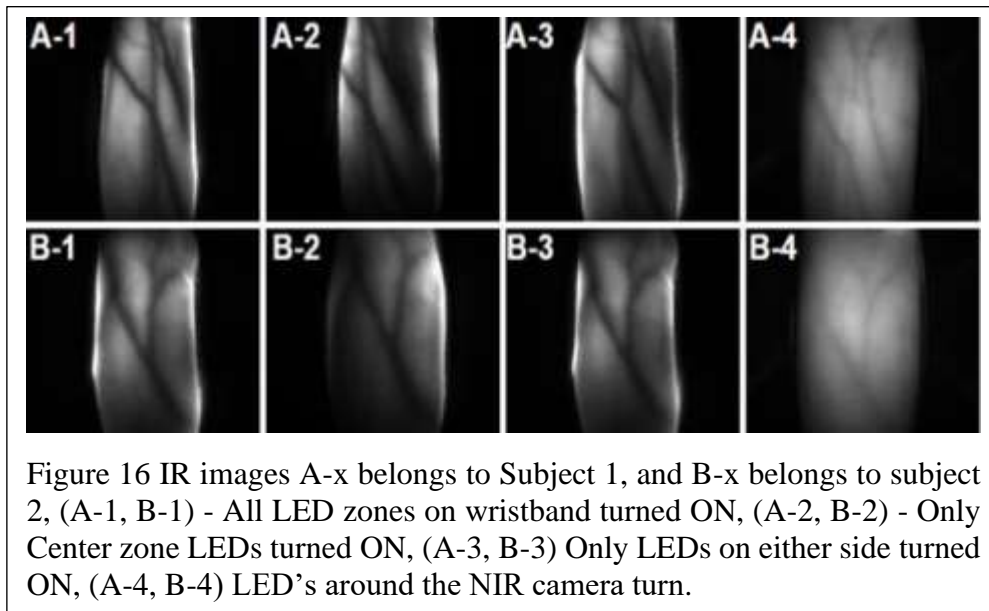
The third configuration encompassed the addition of a photo booth in an effort to get around the restriction stated in the first configuration, which pertained to the exclusive capture of images under nighttime conditions. The incorporation of the photo booth sped up ambient light control and reduced unneeded distractions, enabling image capture in a more controlled environment. Although the introduction of the photo booth reduced the need for night photography and brought about some improvements in image quality, it still had its own inherent drawbacks. Results are shown in figure 15 below.



#### Experiment -4: Final Wristband factor

The third configuration displayed limitations, most notably a lack of sufficient illumination on the palmar side of the wrist and an imperfect execution of the wristband form factor. The fourth and final design was developed to overcome these constraints. Configuration four was created to capture IR photographs without the need for a photo booth, enabling image capture even in daylight. This set-up offered improved illumination covering the entire wrist, providing thorough coverage for the recording of vein patterns. Additionally, a custom 3D holder was created to contain a large number of LEDs and the camera, ensuring ideal alignment and orientation for effective image acquisition. The fourth configuration marked a significant advancement by successfully overcoming the drawbacks present in earlier setups and building a trustworthy and adaptable framework for the acquisition of IR images of the wrist.

The results of several illumination scenarios, including solely refracted, solely reflected, and a combination of both, as seen in the above image, are summarized in figure 16 below. The wristband needed to be wrapped around the lower wrist of the hand in order to capture IR images. The upper part of the custom 3D holder, which held the camera and provided light for the palmar side of the wrist, also needed to be attached with the camera holder.



## 4.2 DoT data

Our initial goal was to use the DoT setup to record pulse photoplethysmography (PPG) signals while the wristband was fastened to the lower wrist area. We ran into complexities related to the complex interaction between PPG signals and the DOT system as our data collection efforts advanced, though. Traditional methods for collecting PPG signals include direct skin contact and are impacted by the pulsatile variations in blood

volume within the blood vessels [14]. As a result of the interaction between infrared light and biological tissue, the DoT setup, on the other hand, indirectly records PPG signals. This presents difficulties in reliably distinguishing PPG signals from background noise and other physiological oscillations. Despite these difficulties, we persisted in collecting data to investigate further useful insights that may be drawn from the DoT setup.

To ensure the reliability and consistency of our data collection efforts and to account for variations in the experimental design and biological characteristics, we obtained two separate samples for each participant (refer figure 17-22 for 3 subject's data with 2 samples each). The collection of numerous samples made it possible to examine the consistency and reproducibility of the measurements, thereby enhancing the dependability of our conclusions. The collected data was then processed, and the Mean Square Error (MSE) was calculated using the data from both sets of samples from each participant. This analysis process gave us enlightening information about the patterns and characteristics present in the collected data. The fields of biometric identification and verification may benefit from these findings.

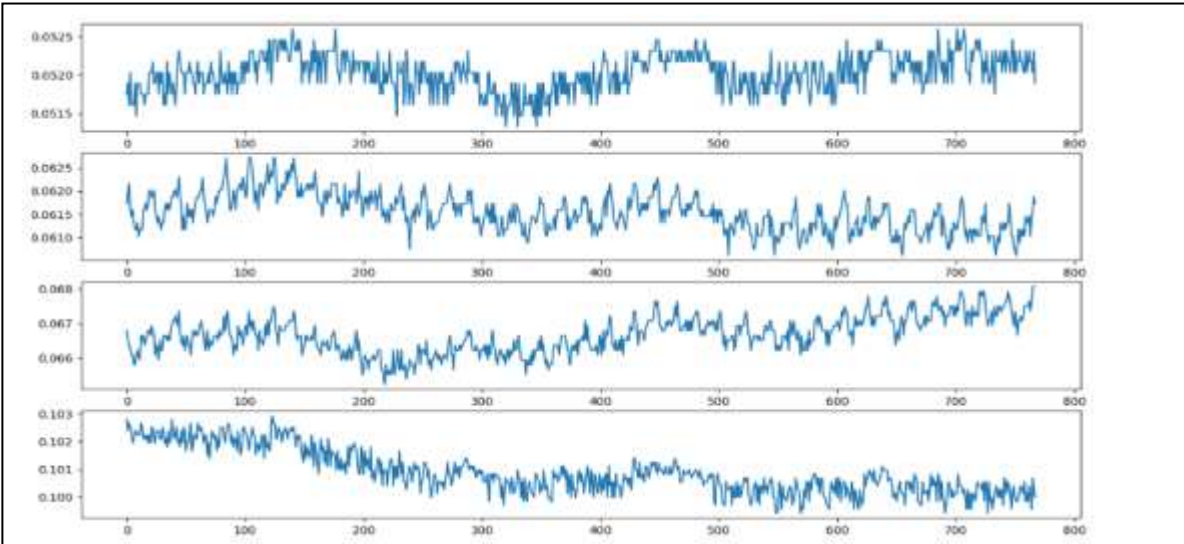


Figure 17 Represents the sample1 of subject 1 for DoT results with four rows; each row represents values from each sensor converted through ADC to digital and taken as graphs. x-axis represents the number of samples taken for 30 seconds and y-axis represents the Voltage value converted. Samples taken when all the location LEDs turned ON (palmar,dorsal,sides) and all the 4 sensors capturing data on different locations of wrist

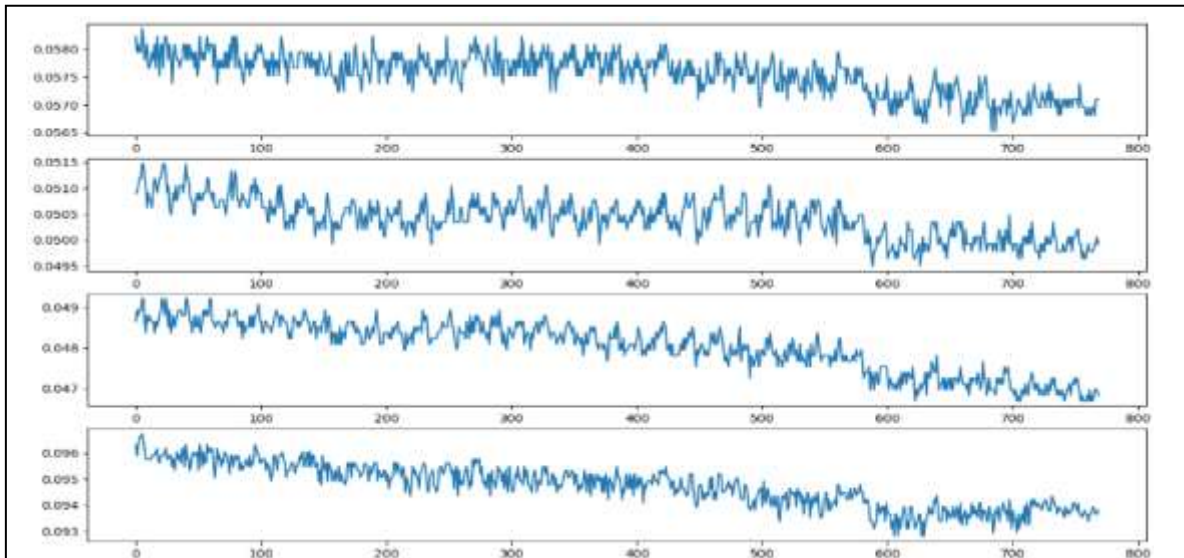


Figure 18 Represents the sample 2 of subject 1 for DoT results with four rows; each row represents values from each sensor converted through ADC to digital and taken as graphs. x-axis represents the number of samples taken for 30 seconds and y-axis represents the Voltage value converted. Samples taken when all the location LEDs turned ON (palmar,dorsal,sides) and all the 4 sensors capturing data on different locations of wrist.



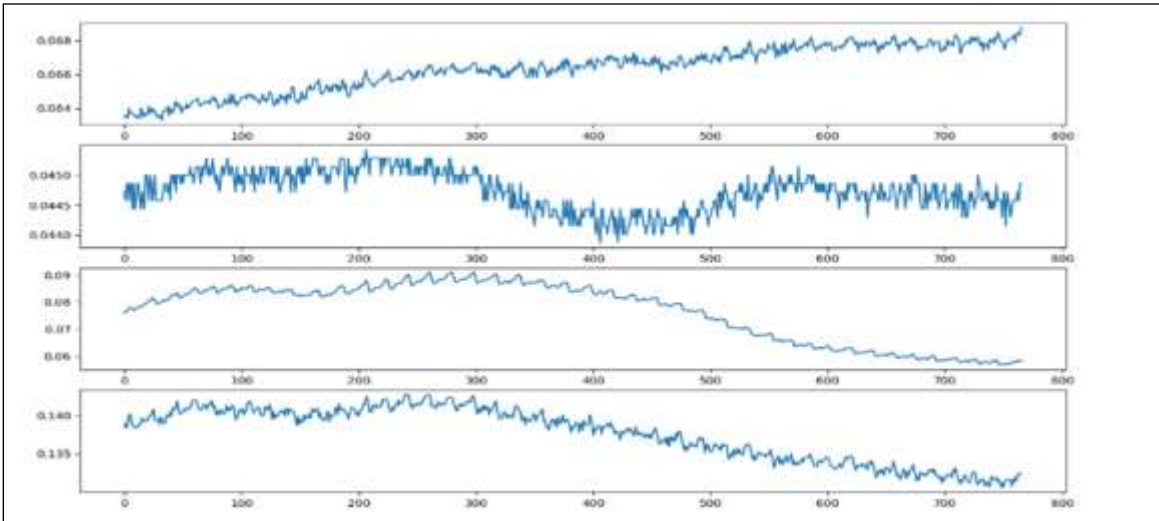


Figure 19 Represents the sample 1 of subject 2 for DoT results with four rows; each row represents values from each sensor converted through ADC to digital and taken as graphs. x-axis represents the number of samples taken for 30 seconds and y-axis represents the Voltage value converted. Samples taken when all the location LEDs turned ON (illumination- palmar,dorsal,sides) and all the 4 sensors capturing data on different locations of wrist

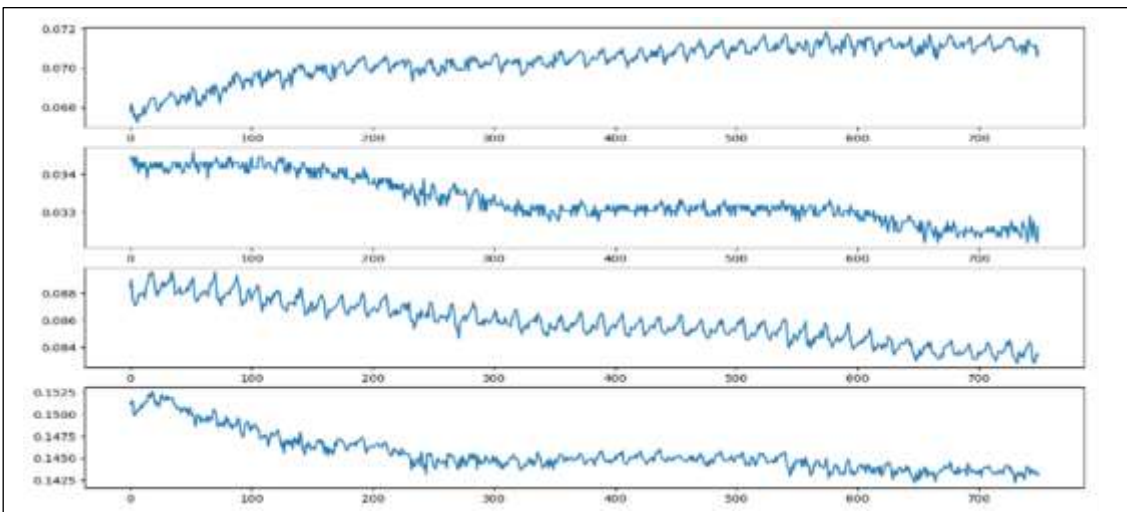


Figure 20 Represents the sample 2 of subject 2 for DoT results with four rows; each row represents values from each sensor converted through ADC to digital and taken as graphs. x-axis represents the number of samples taken for 30 seconds and y-axis represents the Voltage value converted. Samples taken when all the location LEDs turned ON (illumination- palmar,dorsal,sides) and all the 4 sensors capturing data on different locations of wrist

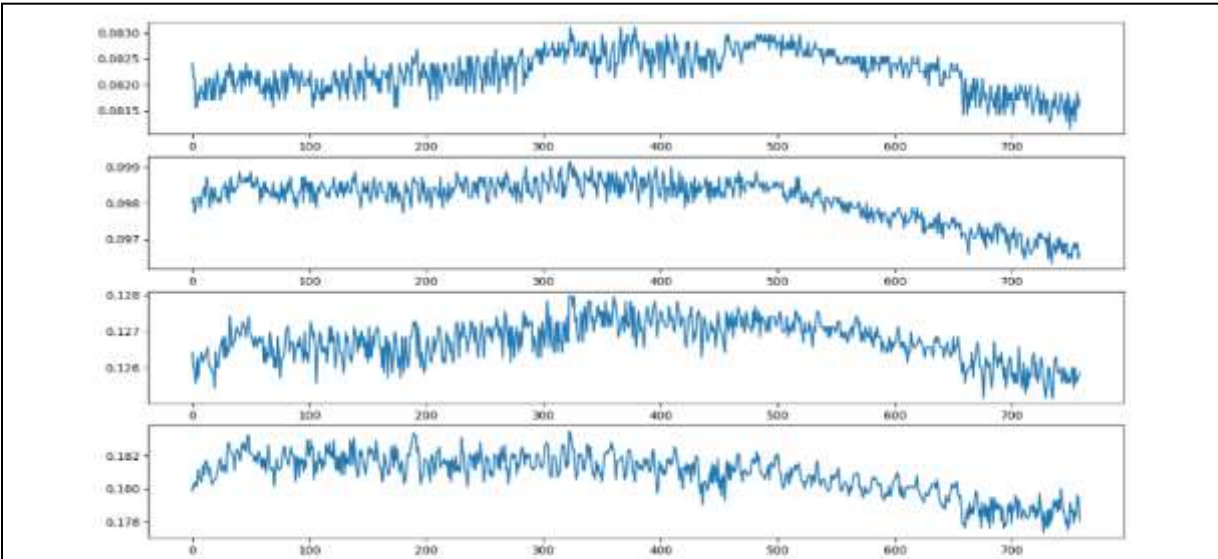


Figure 20 Represents the sample 1 of subject 3 for DoT results with four rows; each row represents values from each sensor converted through ADC to digital and taken as graphs. x-axis represents the number of samples taken for 30 seconds and y-axis represents the Voltage value converted. Samples taken when all the location LEDs turned ON (illumination- palmar,dorsal,sides) and all the 4 sensors capturing data on different locations of wrist

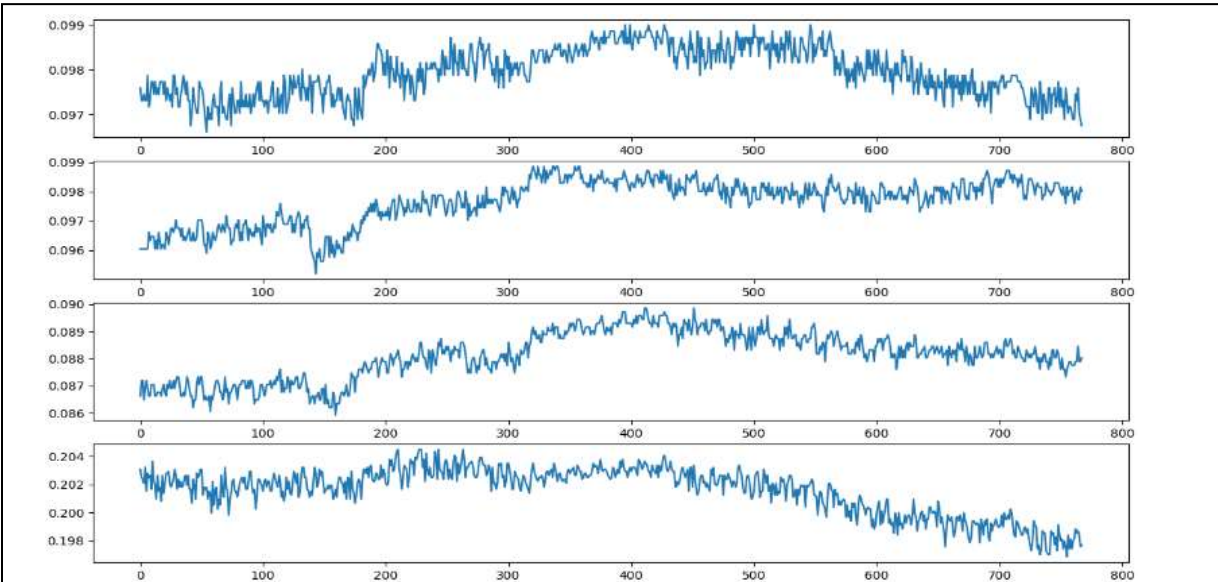


Figure 19 Represents the sample 2 of subject 3 for DoT results with four rows; each row represents values from each sensor converted through ADC to digital and taken as graphs. x-axis represents the number of samples taken for 30 seconds and y-axis represents the Voltage value converted. Samples taken when all the location LEDs turned ON (illumination- palmar,dorsal,sides) and all the 4 sensors capturing data on different locations of wrist

The results from three different subjects, each of whom had two different samples taken, are shown in the graphical representations above. The reliability and reproducibility of the experiments carried out using the provided setup are highlighted by this portrayal. To ensure accurate data collection, each sample was manually obtained over the course of 5 seconds. In addition, we used Mean Square Error (MSE) heat maps, as shown in the following images, to examine the gathered data.

The use of MSE heat maps allowed for a better depiction of the dataset's underlying fluctuations and patterns. The diagonal values in the MSE table, which show the MSE metrics when comparing each sample to itself, are extremely important since they illustrate the intrinsic consistency of each sample. We learned important things about the degree of similarity and dissimilarity between different samples by looking at these MSE values. This analytical method allowed for a comprehensive understanding of the data collected from the DOT setup throughout the length of this experiment.

Table 3 MSE table showing similarity and dissimilarity between tables.

	Subj1, Sample1	Subj2, Sample1	Subj3, Sample1
Subj1, Sample2	6.75E-05	0.0002393	0.001429
Subj2, Sample2	0.0004364	6.33E-05	0.0008852
Subj3, Sample2	0.00169706	0.00115	2.01E-05

The comparison of each sample with itself is illustrated by the diagonal entries in the Mean Square Error (MSE) table above. The diagonal elements (highlighted in red) will exhibit values close to zero due to the fundamental properties of MSE, which measures the squared differences between two samples. In contrast to their own counterparts, the samples' proximity denotes a striking similarity. On the other hand, the non-diagonal elements shown in the MSE table above emphasize the divergence between different samples. Increased non-diagonal values are a sign of diminished similarity since they show observable differences across different samples. We can assess the coherence and variances contained in the dataset by carefully examining the diagonal and non-diagonal values available in the MSE table, enabling a thorough analysis.

## CHAPTER 5

### CONCLUSION AND FUTURE WORK

The main objective of this thesis project was to develop an effective system that was lightweight, energy-efficient, and compact. This system would make it easier to capture infrared (IR) images of wrist veins. The realization of a reliable method for precise and reliable vein pattern detection was the key goal. This mission was distinguished by an iterative series of improvements in which several configurations were carefully designed and improved. The main driving force behind these small modifications was the removal of specific obstacles, which included aspects like controlling ambient light, improving illumination, guaranteeing homogeneity, and achieving a structure that adhered to wristband standards.

#### **5.1 Conclusion**

The systematic improvement of numerous configurations throughout this thesis has resulted in significant advancements in the field of infrared (IR) imaging of wrist veins and DoT data. The result, Configuration 4, successfully overcomes the constraints present in earlier settings. Notably, this arrangement has significantly increased the amount of thorough illumination around all aspects of the wrist, eliminating the need for a photo booth. Additionally, it has achieved a framework that complies with wristbands, resulting in a coordinated and adaptable configuration. The custom 3D holder design ensured exact

placement of the camera and LEDs, enabling painstaking and thorough image collection. DoT data proved the consistency and accuracy for multiple samples of a subject in wristband form factor. By providing a greater understanding of the formulation of effective configurations for the recognition of vein patterns, the findings from this thesis provide a substantial contribution to the field of wrist imaging. The advances made in controlling ambient light, achieving uniform illumination, and improving system design hold promising prospects in a variety of applications, such as biometric recognition systems, healthcare monitoring, and other fields where wrist vein patterns can act as a distinctive and irreplaceable identifier.

## 5.2 Future Work

This analysis has produced promising results for upcoming projects, but it also begs for lines of more research and improvement. Future work will focus on a variety of areas, including improved illumination techniques, improvements in image processing and analysis, real-time monitoring applications, and ergonomic and user experience issues.

Future research may focus on more complex illumination approaches, such the application of adaptive illumination techniques or the integration of multi-wavelength illumination [9], both of which aim to improve the contrast and visibility of restored patterns. The creation of reliable methodologies and algorithms for image processing [13] and analysis, including vein segmentation, feature extraction [20], and pattern recognition, has the potential to improve the accuracy and effectiveness of vein recognition systems.

Real-time monitoring applications, which span areas like continuous authentication and healthcare monitoring, call for investigation. These systems can make use of sophisticated settings and vein identification techniques for practical implementation across a variety of domains. Future system iterations [28] must carefully consider user comfort and operational convenience in order to ensure a pleasant and intuitive experience for both operators and subjects. We have the opportunity to continue enhancing the capabilities, accuracy, and applicability of IR imaging as a method for wrist vein recognition by setting out on a journey of thorough exploration within these domains. This, in turn, has the potential to open up new perspectives for biometric systems and related fields.

## REFERENCE LIST

- [1] S.Lukas, D. Martin, “Retinal Vascular Characteristics,” Part of the *Advances in computer Vision and Pattern Recognition book series(ACVPR)*, 2191-6594, 2020.  
Available: [https://doi.org/10.1007/978-3-030-27731-4\\_11](https://doi.org/10.1007/978-3-030-27731-4_11)
- [2] B. Daniel, C. Francois, H.R Michael: “Infrared and skin: Friend or foe.” *J Photochem. Photobiol. B, Biol.*, 155:78–85, 2016.pen
- [3] S.R Arridge, “Optical tomography in medical imaging,” *Inv. Prob.*, 15 R41 -R93(1999).  
Available: <https://iopscience.iop.org/article/10.1088/0266-5611/15/2/022>
- [4] A. H. Hielscher et al., “Near-infrared diffuse Optical tomography,” *Dis. Markers.*, 18 313 -337(2002). Available: <https://iopscience.iop.org/article/10.1088/0266-5611/15/2/022>
- [5] Y. Guoqiang, D. Turgut, L. Gwen, Z. Chao, C. Britton, Mohler III, R. Emile; Y.G Arjun: “Time-dependent blood flow and oxygenation in human skeletal muscles measured with noninvasive near-infrared diffuse optical spectroscopies.” *J. Biomed. Opt.*, 10(2):024027–024027, 2005.
- [6] B. T. Ton, R. N. J. Veldhuis: “A high quality finger vascular pattern dataset collected using a custom designed capturing device.” In: *Proceedings of the 2013 International Conference on BIOMETRICS (ICB)*, Madrid, Spain. pp. 1–5, 2013.
- [7] AH. Hielscher, AY. Bluestone, GS. Abdoulaev, AD. Klose, J. Lasker, M. Stewart, U. Netz, J. Beuthan: “Near-infrared diffuse optical tomography.” *Dis. Markers.*, 18(5-6):313–337, 2002.



- [8] H. Jiang: “*Diffuse optical tomography: principles and applications*”. CRC press, 2018.
- [9] P. Tome, M. Vanoni, S. Marcel: “On the Vulnerability of Finger Vein Recognition to Spoofing”. In: *IEEE International Conference of the Biometrics Special Interest Group (BIOSIG)*, September 2014.
- [10] J. Xiang, Y. Dong, X. Xue, H. Xiong: “Electronics of a Wearable ECG With Level Crossing Sampling and Human Body Communication.” *IEEE Transactions on Biomedical Circuits and Systems*, 13(1):68–79, 2019.
- [11] J. Galbally-Herrero, J. Fierrez-Aguilar, JD. Rodriguez-Gonzalez, F. AlonsoFernandez, J Ortega-Garcia, M Tapiador: “On the vulnerability of fingerprint verification systems to fake fingerprints attacks.” In: *Proceedings 40th annual 2006 International carnahan Conference on Security Technology*. IEEE, pp. 130–136, 2006.
- [12] A. Ishimaru: *Wave propagation and Scattering in Random Media*, IEEE Press, New York, 1997.
- [13] Alvium® 1800 USB Camera with High-Performance Sony Sensors: , Alvium 1800 U501 NIR. Available online <https://www.edmundoptics.com/p/allied-vision-alvium-1800-u-501m-125-5mp-c-mount-usb-31-nir-monochrome-camera/46910/>
- [14] A. Duncan et al., “A multi wavelength, wideband, intensity modulated optical spectrometer for near infrared spectroscopy and imaging,” *Proc. SPIE*, 1888 248- 257, 1993.
- [15] A. Torricelli et al., “Time domain functional NIRS imaging for human brain mapping,” *NeuroImage*, 85 28 -50, 2014.
- [16] A.H. Hielscher et al., “Near infrared diffuse Optical tomography,” *Dis. Markers*, 18(5-

6), 313 -337(2002).

- [17] B. B. Beard, M. I. Iacono, J. W. Guag and Y. Liu, "A Multi-Frequency 3D Printed Hand Phantom for Electromagnetic Measurements," in *IEEE Electromagnetic compatibility Magazine*, vol. 11, no. 3, pp. 49-54, 3rd Quarter 2022, doi: 10.1109/MEMC.2022.9982572.
- [18] A.B David, M. Dale Anders, A.F. Maria, "Diffuse optical imaging of brain activation: approaches to optimizing image sensitivity, resolution, and accuracy." *NeuroImage*. (Suppl 1): S275–S288, 2004; 23. Available: <https://doi.org/10.1016/j.neuroimage.2004.07.011>
- [19] T. Shimokawa et al., "Hierarchical Bayesian estimation improved depth accuracy and spatial resolution of diffuse optical tomography," *Opt. Express*, 20(18), 20427 -20446, 2012.
- [20] J.P. Culver et al., "Diffuse Optical tomography of cerebral blood flow, oxygenation, and metabolism in rats during focal ischemia," *J. Cereb. Blood Flow Metab.*, 23 911-924, 2003. Available: <https://doi.org/10.1097/01.wcb.0000076703.71231.bb>
- [21] F. Gao, H. Zhao, and Y. Yamada, "Improvement of image quality in diffuse optical tomography by use of full-time resolved data," *Appl. Opt.*, 41(4), 778 -791, 2002.
- [22] J.C. Hebden et al., "Imaging changes in blood volume and oxygenation in the newborn infant brain using three- dimensional optical tomography," *Phys. Med. Biol.*, 49 1117 costs, 2004.
- [23] JES Pascual, J Uriarte-Antonio, R Sanchez-Reillo, MG Lorenz: "Capturing hand or wrist vein images for biometric authentication using low-cost devices." In: *Proceedings*

of the sixth international conference on Intelligent Information Hiding and Multimedia Signal Processing (IIH-MSP 2010), pp 816–819,2010.

- [24] H. Daniel, “Vascular pattern recognition and its application in security-preserving biometric online-banking system,” PhD thesis, PhD dissertation, Department of Information Security, Gjovik University College, 2012.
- [25] RI. Fadhil, LE. George, “*Finger vein identification and authentication system*,” LAP Lambert Academic Publishing, Germany, 2017.
- [26] C. Kauba, B. Prommegger, A. Uhl: “The two sides of the finger—dorsal or palmar—which one is better in finger-vein recognition” In: *Proceedings of the international conference of the Biometrics Special Interest Group (BIOSIG’18)*, Darmstadt, Germany, 2018.
- [27] A. Kumar, Y. Zhou, “Human identification using finger images,” *IEEE Trans Image Process* 21(4):2228–2244, 2012. Available: <http://dx.doi.org/10.1109/TIP.2011.2171697>
- [28] N. Miura, A. Nagasaka, T. Miyatake, “Extraction of finger-vein patterns using maximum curvature points in image profile,” *IEICE Trans Inf Syst* 90(8):1185–1194dor, 2007.
- [29] R. Raghavendra, C. Busch, “Exploring dorsal finger vein pattern for robust person recognition,” In: 2015 *International Conference on Biometrics (ICB)*, pp 341–348, 2015. Available: <https://doi.org/10.1109/ICB.2015.7139059>.
- [30] R. Raghavendra, KB. Raja, J. Surbiryala, C. Busch, “A low-cost multimodal biometric sensor to capture finger veins and fingerprint,” In: *IEEE International Joint Conference*

*on Biometrics (IJCB)*, 2014. IEEE, pp 1–7, 2014.

- [31] R. Raghavendra, S. Venkatesh, K. Raja, C. Busch: “A low-cost multi-finger vein verification system.” In: *proceedings of international conference on Imaging Systems and Techniques (IST 2018)*, Karkow, Poland, 2018.
- [32] K. Shaheed, H. Liu, G. Yang, I. Qureshi, J. Gou, Y. Yin, *A systematic review of finger vein recognition techniques*, Information 9:213, 2018.
- [33] E. Ting, M. Ibrahim, “A review of finger vein recognition system”. *J Telecommun Electron Comput Eng* 10(1–9):167–171, 2018.
- [34] Today BT UK banking customers ready for finger biometrics authentication *Biom. Technol. Today*. 2014(9):3–12. 10.1016/S0969-4765(14)70138-9, 2014. Available: [https://doi.org/10.1016/S0969-4765\(14\)70138-9](https://doi.org/10.1016/S0969-4765(14)70138-9)
- [35] P. Tome, M. Vanoni, S. Marcel, “On the vulnerability of finger vein recognition to spoofing,” In: *IEEE International Conference of the Biometrics Special Interest Group (BIOSIG)*, 2014. Available: <http://publications.idiap.ch/index.php/publications/show/2910>
- [36] B. Ton, “Vascular pattern of the finger: biometric of the future sensor design, data collection and performance verification.,” master’s thesis, University of Twente, 2012.
- [37] C. Zhang, X. Li, Z. Liu, Q. Zhao, H. Xu, F. Su, “The cfvd reflection-type finger-vein image database with evaluation baseline,” In: *Biometric recognition*. Springer, pp 282–287, 2013.

## VITA

Tejaswi Dhandu is born and brought up in India, she received her Bachelor of Technology in Electronics and communication engineering in 2020 from the Jawaharlal Nehru Technological and University in Hyderabad, India. After working at various places as an engineer, and research assistant, working prominently on Embedded systems research, Tele-comm Research. Later in 2021, She joined the Electrical Engineering master's program at the School of Computing and Engineering, University of Missouri-Kansas City. Currently, she is working on her master's thesis, evolution of a Low Swap (Size, weight, and power) Diffuse Optical Tomography and Imaging Techniques for Biometrics.